Bioorg. Med. Chem. 45 (2021) 116315

Contents lists available at ScienceDirect

Bioorganic & Medicinal Chemistry

journal homepage: www.elsevier.com/locate/bmc

Elaboration of a benzofuran scaffold and evaluation of binding affinity and inhibition of *Escherichia coli* DsbA: A fragment-based drug design approach to novel antivirulence compounds

Luke F. Duncan [a,1], Geqing Wang [b,1], Olga V. Ilyichova [c], Rabeb Dhouib [d], Makrina Totsika [d], Martin J. Scanlon [c,e], Begoña Heras [b,*], Belinda M. Abbott [a,*]

[a] Department of Chemistry and Physics, La Trobe Institute for Molecular Science, La Trobe University, Melbourne, VIC 3086, Australia
[b] Department of Biochemistry and Genetics, La Trobe Institute for Molecular Science, La Trobe University, Melbourne, VIC 3086, Australia
[c] Medicinal Chemistry, Monash Institute of Pharmaceutical Sciences, Monash University, 381 Royal Parade, Parkville, VIC 3052, Australia
[d] Centre for Immunology and Infection Control, School of Biomedical Sciences, Queensland University of Technology, Brisbane, Queensland, Australia
[e] ARC Training Centre for Fragment Based Design, Monash Institute of Pharmaceutical Sciences, Monash University, 381 Royal Parade, Parkville, VIC 3052, Australia

ARTICLE INFO

Keywords:
Fragment-based drug discovery
Benzofuran
Oxidoreductase
DsbA
Enzyme inhibition
Antivirulence

ABSTRACT

Bacterial thiol-disulfide oxidoreductase DsbA is essential for bacterial virulence factor assembly and has been identified as a viable antivirulence target. Herein, we report a structure-based elaboration of a benzofuran hit that bound to the active site groove of *Escherichia coli* DsbA. Substituted phenyl groups were installed at the 5- and 6-position of the benzofuran using Suzuki-Miyaura coupling. HSQC NMR titration experiments showed dissociation constants of this series in the high μM to low mM range and X-ray crystallography produced three co-structures, showing binding in the hydrophobic groove, comparable with that of the previously reported benzofurans. The 6-(*m*-methoxy)phenyl analogue (**2b**), which showed a promising binding pose, was chosen for elaboration from the C-2 position. The 2,6-disubstituted analogues bound to the hydrophobic region of the binding groove and the C-2 groups extended into the more polar, previously un-probed, region of the binding groove. Biochemical analysis of the 2,6-disubsituted analogues showed they inhibited DsbA oxidation activity *in vitro*. The results indicate the potential to develop the elaborated benzofuran series into a novel class of antivirulence compounds.

1. Introduction

Bacterial infections are becoming a serious threat to global health. The rapid emergence and spread of antibiotic resistant bacteria coupled with a drying pipeline of new antibiotics is threatening our ability to control drug resistant infections. If no action is taken, we are heading for a post-antibiotic era where common infections are no longer treatable.[1] In the US alone, 2.8 million people acquire antibiotic-resistant infections annually with more than 35,000 deaths claimed.[2] With the reduction in efficacy of current therapeutics, new classes of antibiotics with novel mechanisms of action are urgently needed. One strategy to prevent or reduce bacterial resistance is to develop antimicrobials that target virulence rather than viability.[3–5] This new paradigm for targeting bacterial infections offers a number of advantages over conventional antibiotics, including a large repertoire of unexplored virulence targets, a reduced selective pressure on pathogenic bacteria to develop resistance and preservation of the host microbiota.[3]

Pathogenic bacteria rely on virulence factors to colonize the host, establish infections and cause disease.[6] Examples of virulence factors include proteins that make up fimbrial and non-fimbrial adhesins, secreted toxins, secretion systems and motility organelles.[4] Common among many of these virulence proteins is the requirement of enzymatic oxidative folding to achieve their functional conformation.[7,8] This task is undertaken by the thiol-disulfide oxidoreductase DsbA, a thioredoxin-like protein with a redox active CXXC motif that introduces disulfide bonds to cysteine pairs in unfolded substrates.[7,9] As DsbA folds a broad range of virulence factors, lack of functional DsbA has pleiotropic effects on multiple virulence-associated phenotypes and therefore represents an

* Corresponding authors.
E-mail addresses: B.Heras@latrobe.edu.au (B. Heras), B.Abbott@latrobe.edu.au (B.M. Abbott).
[1] Both authors contributed equally to this work.

https://doi.org/10.1016/j.bmc.2021.116315
Received 20 May 2021; Received in revised form 15 July 2021; Accepted 16 July 2021
Available online 22 July 2021

attractive approach to inhibit bacterial virulence.[10] The prototypical *Escherichia coli* (*Ec*) DsbA, the best characterised DsbA enzyme, consists of a thioredoxin domain and an inserted α-helical domain. A notable feature of *Ec*DsbA is the presence of a hydrophobic groove adjacent to the CXXC active site, which serves as the binding site for redox partner DsbB and substrates (Fig. 1A).[11,12] During the disulfide bond catalysis, the active site cysteines of DsbA become reduced when the substrate is oxidised and the membrane-bound partner enzyme DsbB restores DsbA to its oxidised state. As the hydrophobic groove is critical for redox interactions, a range of peptide and small molecule inhibitors have been developed to disrupt DsbA activity by targeting the hydrophobic groove.[13–16]

In recent decades fragment-based drug discovery (FBDD) has emerged as a powerful alternative method to conventional high-throughput screening approaches for drug lead discovery and development.[17] Due to the small size (<300 Da) and lack of complexity of the compounds typically found in fragment screening libraries, their structures are less likely to contain motifs that will sterically hinder target binding, considerably increasing the likelihood of hit identification.[18] A fragment-based screening approach combining X-ray crystallography and NMR, was previously used to identify the first non-peptide *Ec*DsbA inhibitors.[14] This work underscores the utility of FBDD to tackle challenging targets like DsbA, where the active site comprises a shallow and extended hydrophobic groove involved in protein-protein interactions. More recently, we reported a new class of *Ec*DsbA inhibitors identified from a fragment library.[19] Using X-ray crystallography we were able to show that benzofuran derivatives bound to the hydrophobic groove of *Ec*DsbA (Fig. 1B). Furthermore, using HSQC NMR titration we determined that 6-phenoxy and 6-benzyl analogues were the strongest binders.[19] Herein we report the chemical synthesis of 2-, 5- and 6-substituted benzofuran derivatives and their biophysical characterisation and *in vitro* analysis of *Ec*DsbA inhibition. We have generated, guided by X-ray crystallography and NMR spectroscopy, benzofurans exhibiting improved *in vitro* inhibition of *Ec*DsbA.

2. Results and discussion

2.1. Chemical synthesis

For optimisation of the binding capacity of the previously identified benzofuran hits, we explored substitutions at the 5- and 6-position as possible sites for elaboration (Fig. 1B). Precursors **1a-c**, which were synthesised as previously described,[19] were substituted at C-5 and C-6 via Suzuki-Miyaura coupling with boronic acids (Scheme 1). Compounds **2a-c** were isolated in low to moderate yields after a difficult purification using chromatography and recrystallisation. Similarly, C-5 substituted **2d** was isolated in low yield after purification by RP-HPLC. Phenylboronic acid was also coupled to **1a** but the cross-coupled

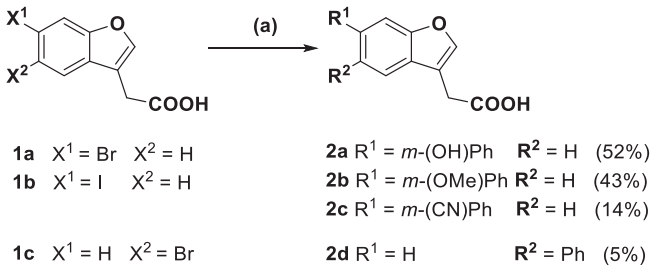

1a X^1 = Br X^2 = H
1b X^1 = I X^2 = H
1c X^1 = H X^2 = Br

2a R^1 = *m*-(OH)Ph R^2 = H (52%)
2b R^1 = *m*-(OMe)Ph R^2 = H (43%)
2c R^1 = *m*-(CN)Ph R^2 = H (14%)
2d R^1 = H R^2 = Ph (5%)

Scheme 1. C-5 and C-6 substitution of acids **1a-c** via Suzuki-Miyaura cross-coupling (isolated yields shown in brackets). *Reagents and conditions*: (a) R-B$(OH)_2$, CsF, Pd(dppf)Cl_2, CH_3CN:H_2O (4:1), 90 °C, 16–24 h.

product could not be isolated from the crude reaction mixture. To aid purification, an alternate two-step synthetic route using methyl ester **3a** or **3b** was employed (Scheme 2).

Aryl bromide **3a** was coupled to phenylboronic acid via Suzuki-Miyaura coupling and the cross-coupled product **4a** was able to be

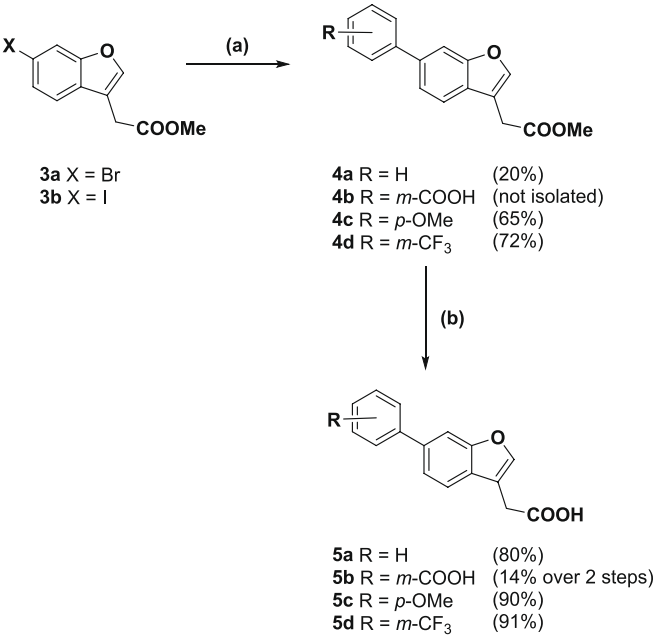

3a X = Br
3b X = I

4a R = H (20%)
4b R = *m*-COOH (not isolated)
4c R = *p*-OMe (65%)
4d R = *m*-CF_3 (72%)

5a R = H (80%)
5b R = *m*-COOH (14% over 2 steps)
5c R = *p*-OMe (90%)
5d R = *m*-CF_3 (91%)

Scheme 2. C-6 substitution of methyl esters **3a** and **3b** via Suzuki-Miyaura cross-coupling (isolated yields shown in brackets). *Reagents and conditions*: (a) R-Ph$(BOH)_2$, CsF, Pd(dppf)Cl_2, CH_3CN:H_2O (4:1), 90–120 °C, 0.25–28 h. (b) 2 M NaOH, CH_3OH:CH_2Cl_2 (9:1), r.t, 16 h.

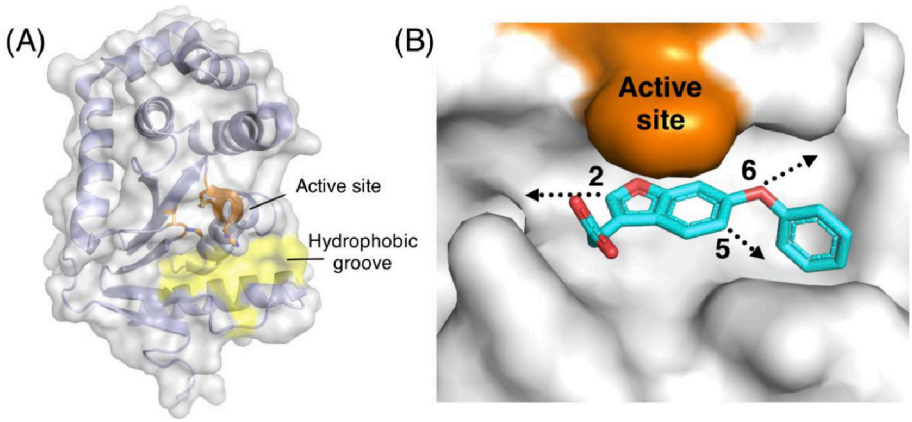

Fig. 1. Crystal structures of *Ec*DsbA in apo and compound-bound forms. (A) Crystal structure of oxidised *Ec*DsbA (PDB ID: 1FVK). The Cys30-Pro31-His32-Cys33 motif and *cis*-Pro loop (Val150-*cis*-Pro151) of the active site are presented as orange sticks. The hydrophobic groove adjacent to the active site is shaded in yellow. (B) Crystal structure of *Ec*DsbA in complex with the best benzofuran analogue from the previous series (PDB ID: 6POI).[19] Growth vectors used for compound elaboration in this study are indicated by dashed arrows of the 2-,5- and 6-positions of the benzofuran core. The active site is shaded in orange.

isolated via chromatography albeit in low yield. Following this, **4a** was hydrolysed to the desired acid **5a**. Similarly, *m*-carboxyphenylboronic acid was coupled to **3a**, however chromatography could not separate the homo-coupled boronic acid by-product from cross-coupled **4b**. Subsequent ester hydrolysis of impure **4b** allowed for isolation of the desired acid **5b** by chromatography in 14% yield over two steps. The 6-iodobenzofuran **3b** was used for synthesis of the *p*-methoxyphenyl and *m*-trifluoromethylphenyl derivatives **5c** and **5d**. The increased reactivity of the aryl iodide coupling partner resulted in superior yields and, furthermore, reaction times were dramatically reduced by heating the reaction by microwave irradiation.

With the aim to elaborate the benzofuran scaffold from the 2-position (Fig. 1B), compound **3a** was brominated using bromine in acetic acid (Scheme 3). The desired 2,6-dibromo **6a** formed in a favourable 1:0.4 ratio with regioisomer **6b** according to ^{1}H NMR. The regioisomers were inseparable by chromatography but recrystallisation from isopropanol exclusively afforded the desired 2,6-dibromo isomer **6a** in a 52% yield. To investigate the reactivity of the 2-position versus the 6-position, **6a** was coupled to an equimolar amount of phenylboronic acid via Suzuki-Miyaura coupling which resulted in a mixture of regioisomers **7a** and **7b** as well as di-substituted **7c**. These compounds were separated via RP-HPLC. While the preferred formation of **7b** indicated there was slightly higher reactivity at the 2-position, it was not significant enough to exploit. The 2-phenyl-6-bromo isomer was hydrolysed to acid **8a** in quantitative yield.

To improve selectivity of the coupling reaction, the bromination and subsequent substitution was repeated on the more reactive 6-iodobenzofuran **3b** (Scheme 4). As with compound **3a**, bromination afforded a mixture of regioisomers **9a** and **9b** which required recrystallisation from isopropanol to isolate the desired isomer **9a** in a 57% yield. With the appropriate coupling partner in hand, the increased reactivity of the aryl iodide over the bromide could be exploited to selectively install an aromatic group at C-6. Compound **9a** was coupled with one equivalent of *m*-methoxyphenylboronic acid in an attempt to avoid di-substitution. The reaction was heated to 80 °C under microwave irradiation, which allowed a shorter reaction time of 1 h. The cross-coupling proceeded with far superior selectivity at the more reactive 6-iodo position and

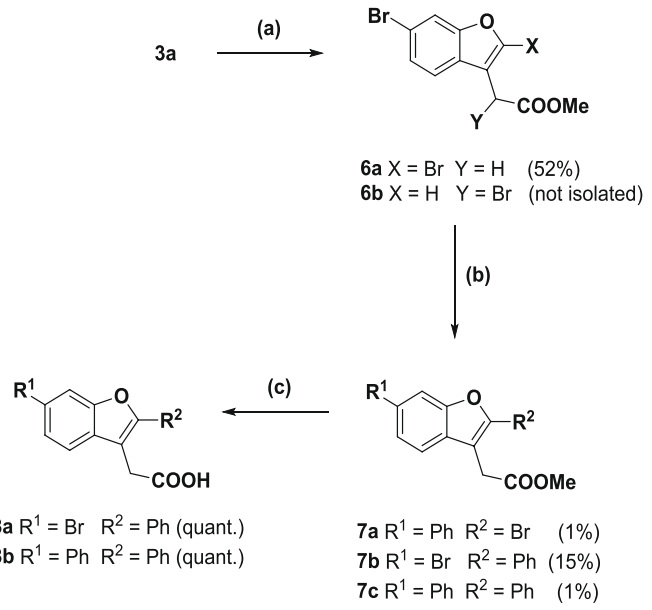

Scheme 3. Suzuki-Miyaura coupling of phenylboronic acid to 2,6-dibromo compound **6a** and subsequent ester hydrolysis (isolated yields shown in brackets). *Reagents and conditions*: (a) Br_2, CH_3COOH, r.t, 3 h; (b) R-PhB$(OH)_2$, CsF, Pd(dppf)Cl_2, CH_3CN:H_2O (4:1), 90 °C, 24 h. (c) 2 M NaOH, CH_3OH:CH_2Cl_2 (9:1), r.t, 16 h.

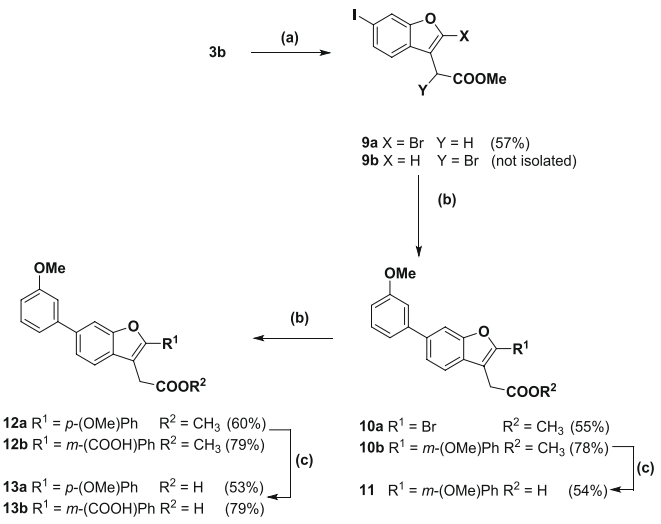

Scheme 4. Formation of 2,6-disubsituted benzofurans via Suzuki-Miyaura cross-coupling (isolated yields shown in brackets). *Reagents and conditions*: (a) Br_2, CH_3COOH, r.t, 3 h; (b) R-PhB$(OH)_2$, CsF, Pd(dppf)Cl_2, CH_3CN:H_2O (4:1), 80–120 °C MW, 15–60 m; (c) 2 M NaOH, CH_2Cl_2:CH_3OH (9:1), r.t, 16 h.

only a minor amount of a 2,6-disubstituted by-product was observed, which could be separated via chromatography to afford **10a** in a 55% yield. Repeating the reaction using four equivalents of *m*-methoxyphenyl boronic acid led to the disubstituted product **10b** in good yield, which was hydrolysed to acid **11.** The 2-bromo position of **10a** was then substituted with *p*-methoxyphenylboronic acid and *m*-carboxyphenylboronic acid by Suzuki-Miyaura coupling to afford **12a** and **12b** in fair to high yields. The reactions were heated to 120 °C under microwave irradiation for 15 min. The methyl esters of **12a** and **12b** were hydrolysed using sodium hydroxide in methanol:DCM (1:9) to give acids **13a** and **13b** respectively in good to high yields.

2.2. Structure-guided elaboration of benzofuran as DsbA inhibitors

To guide chemical elaboration of the benzofuran series as DsbA inhibitors, we developed a fast and robust crystallography protocol for compound soaking, data acquisition and structure determination.[14] Synthesised compounds were tested for their ability to bind DsbA by three ligand-detected 1D NMR methods: saturation-transfer difference (STD)[20], Carr-Purcell-Meiboom-Gill (CPMG)[21] and water-ligand observed via gradient spectroscopy (waterLOGSY)[22] (Table 1, assessment criteria has been detailed in section 4.5). We and others have shown that compounds validated using multiple ligand-detected NMR experiments, have a higher likelihood of yielding the co-crystal structures.[14,23] Therefore, these experiments provided a benchmark to prioritise compounds for crystal soaking and binding affinity determination. As exemplified in Fig. 2A, the binding of **5a** to DsbA was validated in all three ligand-detected NMR experiments. Comparison of the 1D ^{1}H NMR spectrum of **5a** and the STD spectrum of **5a** + DsbA showed magnetization transfer from DsbA to the aromatic resonances of **5a**. The waterLOGSY NMR spectrum showed that the aromatic resonances of **5a** became less negative in the presence of DsbA compared to **5a** alone. The CPMG NMR spectrum (τ = 350 ms) of **5a** showed attenuation of its aromatic resonances in the presence of DsbA.

In previous work we introduced various aryl and alkyl groups with methylene, ether and amino bridges at C-6 of the benzofuran scaffold.[19] X-ray crystallography and NMR spectroscopy showed that the binding mode and affinity were dependent on the size and substitution of the group. Noteworthy was the installation of a *p*-anisidine moiety which resulted in the flipping and shift of the benzofuran core which interrupted the important π-π stacking interactions with His32 of DsbA and compromised binding affinity.[19] This outcome suggests that a large

Table 1
Biophysical and biochemical characterisation of benzofuran analogues.

I.D	Structure	Crystal Structure obtained	wLOGSY	CPMG	STD	Dose response HSQC K_D (μM)	Ligand efficiency (kcal mol^{-1} HAC^{-1})
2a	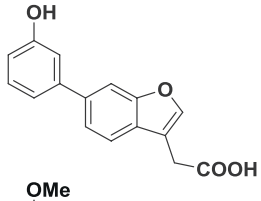	Yes	Pass	Pass	Pass	830 ± 250	0.21
2b	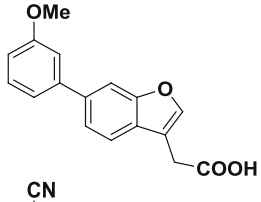	Yes	Pass	Pass	Pass	1100 ± 300	0.19
2c	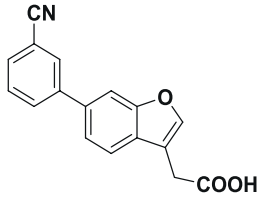	No	Pass	Pass	Pass	2300 ± 800	0.17
2d	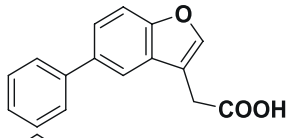	No	Pass	Pass	Pass	820 ± 140	0.22
5a	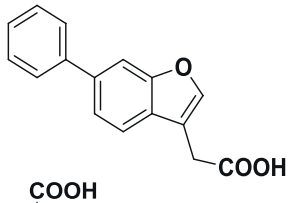	Yes	Pass	Pass	Pass	1137 ± 178	0.21
5b	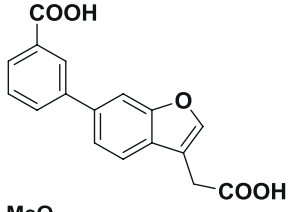	No	Fail	Pass	Fail	≫ 1000	≫0.19
5c	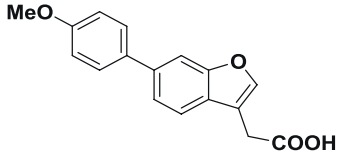	No	Pass	Pass	Fail	460 ± 70	0.22
5d	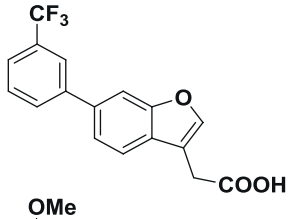	No	Pass	Pass	Pass	403 ± 69	0.20
11	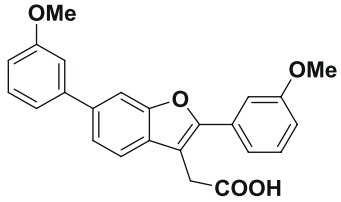	Yes	Pass	Pass	Fail	531 ± 281	0.15
13a		Yes	Fail	Fail	Pass	274 ± 34	0.17

(*continued on next page*)

Table 1 (*continued*)

I.D	Structure	Crystal Structure obtained	wLOGSY	CPMG	STD	Dose response HSQC K_D (μM)	Ligand efficiency (kcal mol^{-1} HAC^{-1})
13b	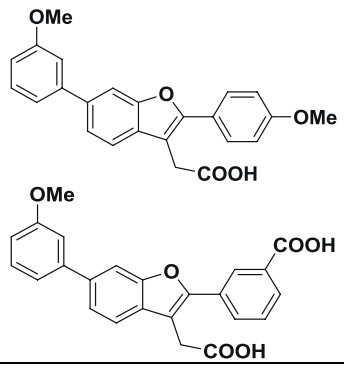	Yes	Pass	Pass	Pass	978 ± 99	0.14

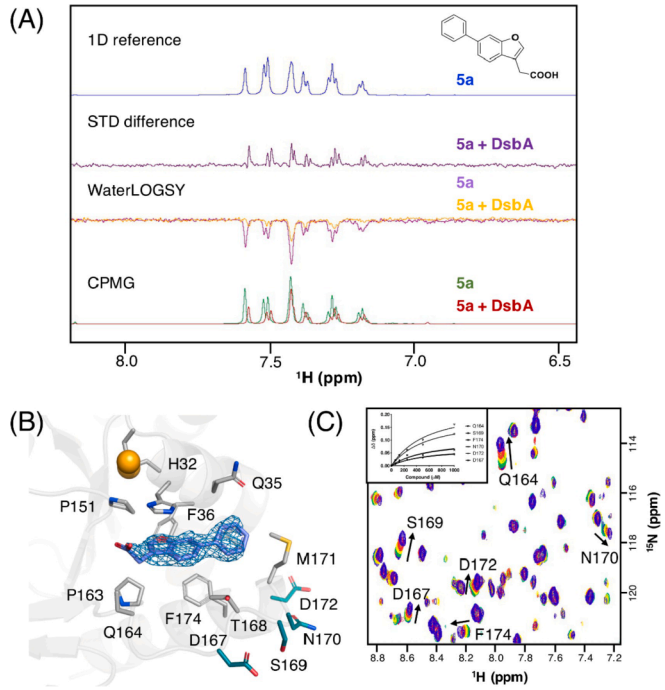

Fig. 2. Overview of biophysical and structural characterisation of benzofuran analogues. (A) Binding of **5a** to *Ec*DsbA was evaluated by a series of ligand-detected NMR spectroscopy including STD, waterLOGSY and CPMG. (B) Crystal structure of **5a** bound to *Ec*DsbA. Simulated annealing omit σ_A-weighted mFo-DFc electron density map for **5a** is contoured at 2.5σ and shown as blue mesh. Residues within 4 Å of **5a** are presented as grey sticks. Residues that were perturbed in the HSQC spectra but not within 4 Å of **5a** are presented as green sticks. (C) A portion of the ^{1}H-^{15}N HSQC spectra of ^{15}N-labelled *Ec*DsbA showing chemical shift perturbation (CSP) upon the titration of increasing concentrations of **5a** (0, 0.0625, 0.125, 0.25, 0.5 and 1 mM). The direction of the CSP is indicated by black arrows. Insert shows the equilibrium dissociation constant (K_D) determination of **5a** by measurement of CSP as a function of compound concentration. Full HSQC spectra are shown in supplementary Fig. S1.

moiety cannot be accommodated in the right-hand-side (RHS) pocket of the hydrophobic groove lined by residues Gln35, Leu40, Thr168, Met171 and Phe174 (Fig. 1C). In this work, to further optimise the interactions in the RHS pocket, we substituted the benzofuran moiety with a phenyl group to generate compound **5a**. A crystal structure of *Ec*DsbA in complex with **5a** was determined at 1.83 Å resolution. Data collection and refinement statistics are listed in the supplementary Table S1. $2F_o$-F_c electron density maps and omit maps of these compounds are shown in supplementary Fig. S2. The co-structure revealed that the benzofuran core formed π-stacking interactions with His32 and the carboxylic acid was oriented towards the more polar region of the binding groove, which resembles previously reported co-structure of aniline analogues.[19] Due to the reduced size of the phenyl group relative to aniline at C-6 of the benzofuran, the RHS pocket of the hydrophobic binding groove was only partially occupied (Fig. 2B). Based on this observation, a series of functional groups were introduced in the *meta* and *para* positions of 6-phenyl in **2a-c** and **5b-d** to occupy this pocket. Most of these compounds passed all three ligand-detected NMR experiments, except **5b** only showed binding in the CPMG experiment and **5c** exhibited binding in both wLOGSY and CPMG experiments but not in the STD experiment (Table 1). Among these analogues, only **2a** and **2b** produced good electron density in the resulting crystal structures. The co-structure (*i.e.* crystal structure of the protein-compound complex) of **2b** confirmed the design strategy and uncovered the high complementarity between the 6-(*m*-methoxy)phenyl group and the pocket (Fig. 3A). It is interesting to note that the side chain of M171, which defines one end of the hydrophobic groove, could re-orientate to accommodate the bound molecules. The *m*-hydroxy **2a** analogue produced a co-structure comprising two ligands bound to the hydrophobic groove in a head-to-tail manner (Supplementary Fig. S3). This is possibly a crystallography artefact due to the high concentration of ligands used on soaking and has been observed in other reported DsbA-compound complexes.[14] To interrogate the 5-position of the benzofuran a phenyl group was introduced in **2d**. Although **2d** passed all three ligand-detected NMR experiments, no co-crystal structure was obtained to support further elaboration from this position.

In an attempt to expand into the left-hand-side (LHS) of the hydrophobic groove, a phenyl group was installed at the C-2 position of the benzofuran core in compound **7b**. The lack of an aromatic substituent at C-6 resulted in a shift of the benzofuran scaffold further into the hydrophobic end of the binding groove, possibly weakening the π-stacking interaction with His32 (Fig. 3A). Nevertheless, the co-structure validated the 2-position as an appropriate vector to grow the scaffold into more polar region of the binding groove. As shown earlier, the co-structure of **2b** highlighted the favourable binding pose of the compound and favourable interactions of the (*m*-methoxy)phenyl group at the C6-position of the benzofuran, therefore we decided to use this pharmacophore in the next round of elaboration. To further explore the polar region in the LHS of the groove, methoxy and carboxy groups were introduced in the *meta* and *para* positions of the 2-phenyl group in compounds **11**, **13a** and **13b**. *Ec*DsbA crystals soaked with these compounds all diffracted between 1.99 and 2.30 Å resolution. Data collection and refinement statistics are listed in the supplementary Table S1. $2F_o$-F_c electron density maps and omit maps of these compounds are shown in supplementary Fig. S2. The co-crystal structures of **11**, **13a** and **13b** bound to *Ec*DsbA (Fig. 3B-D) showed that these compounds adopted

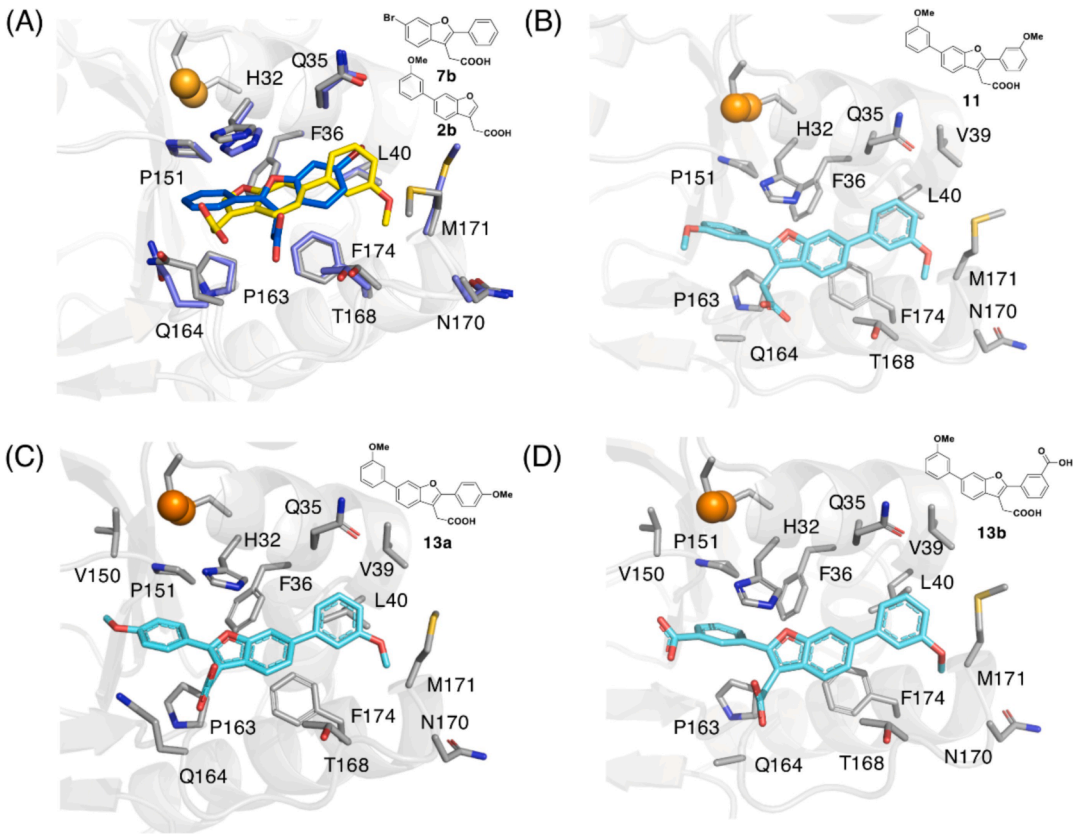

Fig. 3. Crystal structure-guided elaboration of benzofuran analogues as *Ec*DsbA inhibitors. (A) Structure overlay of the **2b**(yellow)-*Ec*DsbA complex and the **7b** (blue) -*Ec*DsbA complex. Residues within 4 Å of **2b** are presented as purple sticks and residues within 4 Å of **7b** are presented as grey sticks. (B-D) Crystal structures of **11** (B), **13a** (C) and **13b** (D) bound to *Ec*DsbA. Residues within 4 Å of the binders are presented as grey sticks. The sulfur atoms of the active site disulfide bond are presented as orange spheres. Residues within 4 Å of compounds are shown as grey sticks. Chemical structures of compounds are shown in the upper right part of each figure.

a similar binding pose in the hydrophobic groove with the benzofuran core forming π-stacking interactions with His32 and Phe174 of DsbA. As intended, the 2-(*m*-methoxy)phenyl group of **11**, 2-(*p*-methoxy)phenyl group of **13a** and the 2-(*m*-carboxy)phenyl group of **13b** were found to extend to the more polar region of the binding groove. Although no polar interactions formed between the compounds and the protein, the derivatised phenyl groups seem to be stabilised by a cluster of hydrophobic residues including Pro163, Phe36 and *cis*-Pro151. Their binding modes are in consensus with previously reported DsbA inhibitors such as phenylthiazole, diaryl ether and phenylthiophene[14,15,19,24] and highlight that DsbA is highly capable of binding hydrophobic molecules without engaging many specific polar interactions. Among these interacting residues, Phe36, His32 and *cis*-Pro151 are highly conserved across DsbA homologues[15] and the latter two are also critical for DsbA redox activity,[25] suggesting that these compounds may exert an inhibitory activity on DsbA.

2.3. Biophysical evalution of benzofuran analogues

Binding of benzofuran analogues to DsbA was further characterised using 2D ^{1}H-^{15}N heteronuclear single quantum coherence (HSQC) spectroscopy by monitoring the chemical shift perturbation (CSP) of cross peaks upon addition of 1 mM compound. These experiments allowed mapping the binding site onto DsbA for compounds like **2c**, **5b**, **5c** and **5d,** for which co-crystal structures could not be determined. The CSP patterns showed that for all compounds tested, the most dramatic changes were observed for cross peaks assigned to Gln164, Ser169, Phe174 and Asn170. (Fig. 4) The majority of the perturbed residues were located around the hydrophobic groove, involved in DsbB binding, and on the flexible *cis*-Pro loop, which is required for substrate recognition and binding.[12,26] It should be noted that although the co-crystal structures showed π-stacking of the benzofuran analogues with His32, this residue is not observed in the HSQC spectrum of apo *Ec*DsbA and therefore its CSP cannot be measured.

Ligands that induced appreciable CSP (>0.04 ppm) of at least three residues were selected for dose-response titration over a concentration gradient to calculate the equilibrium dissociation constant (K_D) (Table 1). Intriguingly, the additional interactions formed by the *m*-methoxy group of **2b** in the hydrophobic pocket did not translate to improved binding affinity. **2b** and **5a** exhibited identical binding affinity, 1100 ± 200 μM and 1100 ± 300 μM, respectively. At the *meta* position of the 6-phenyl group, hydroxy (**2a**) substitution produced similar affinity (830 ± 250 μM) as **5a** and **2b**; trifluoromethyl substitution (**5d**) improved the affinity to 403 ± 69 μM; whilst cyano (**2c**) and carboxy substitution (**5b**) dramatically reduced the binding affinity to above 2 mM. At the *para* position of the 6-phenyl group, methoxy (**5c**) enhanced the binding affinity to 460 ± 70 μM. Elaboration at the C5 position of the benzofuran core produced compound **2d**, which displayed similar binding affinity as C6-substituted **5a**. Among these analogues, 6-(*p*-methoxy)phenyl derivative **5c** and 6-(*m*-trifluoro)phenyl derivative **5d** showed the highest affinities but unfortunately failed to produce interpretable electron density in the crystal structures. For this reason, 6-(*m*-methoxy)phenyl derivative **2b**, which had a K_D of 1100 ± 300 μM but displayed clear electron density in the co-structure, was chosen for elaboration from the C-2 position.

Among the three 2,6-disubstituted analogues, **13a** produced the highest binding affinity of 274 ± 34 μM, while **11** and **13b** produced the binding affinity of 531 ± 281 μM and 978 ± 99 μM, respectively. (Fig. 4)

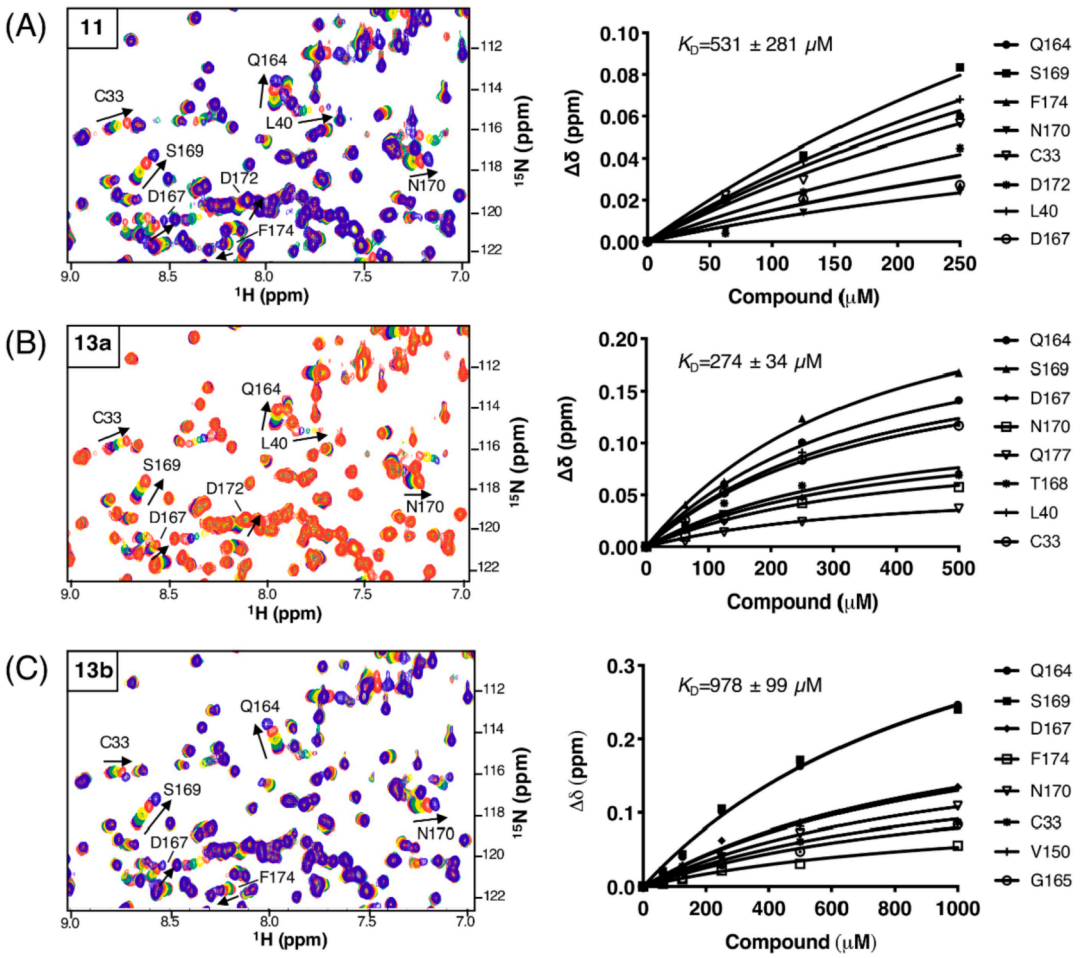

Fig. 4. NMR characterisation of elaborated benzofuran analogues 11 (A), **13a** (B) and **13b** (C) **binding to DsbA.** Panel (A-C): Left: A portion of the ^{1}H-^{15}N HSQC spectra of ^{15}N-labelled *Ec*DsbA showing chemical shift perturbation (CSP) upon the titration of increasing concentration of **11**, **13a** and **13b** (0 (red), 0.0625 mM (blue), 0.125 mM (green), 0.25 mM (yellow), 0.5 mM (red) and 1 mM (blue)). Right: the equilibrium dissociation constant (K_D) determination of **11**, **13a** and **13b** by measurement of CSP as a function of compound concentration. The K_D value is shown as K_D ± error of fit.

It should be noted, precipitation of **11** was observed at 0.5 and 1 mM, therefore only CSP at concentrations < 0.5 mM were used for K_D determination. Similarly, **13a** was not soluble at 1 mM, therefore only CSP at concentrations < 1 mM were used for K_D determination. The affinity difference of these compounds was supported by LIGPLOT analysis of their co-structures, which showed that **13a** makes the highest number (n = 47) of interactions with DsbA while **13b** makes the lowest number (n = 34) of contacts with DsbA. The LIGPLOT analysis of the three compounds is shown in supplementary Fig. S4, lists of detailed interactions are presented in Table S2.

2.4. Biological evalution of benzofuran analogues

The binding of 2,6-disubtituted benzofuran analogues to the DsbA hydrophobic groove and their improved binding affinities relative to the parent compounds[14] prompted us to investigate the ability of compounds **13a**, **13b** and **11** to inhibit DsbA redox activity using a standard peptide oxidation assay (POA). As illustrated in Fig. 5, compound **13a** inhibited DsbA activity *in vitro* in a concentration-dependent manner, producing an IC_{50} of 140 ± 13 μM. Its inhibitory activity correlates well with its NMR K_D value (274 ± 34 μM). Compounds **11** and **13b** however were found to quench fluorescence signals in the assay. As fluorescence signal correlates with DsbA activity, this quenching effect resulted in artificially enhanced inhibition (Supplementary Fig. S5) and therefore it was not possible to reliably determine IC_{50} for these two compounds. It is likely that **11** and **13b** formed assay interfering aggregates.[42] The

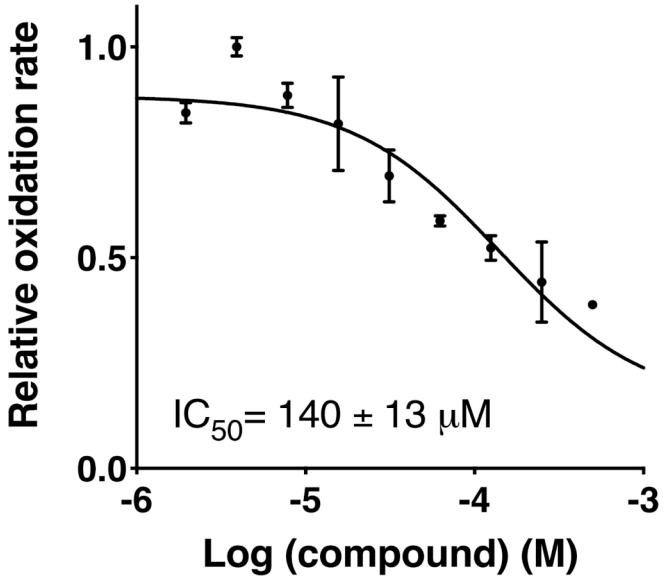

Fig. 5. Concentration-dependent inhibition of *Ec*DsbA oxidation activity by 13a determined using a peptide oxidation assay. IC_{50} is shown as mean ± standard error of mean (SEM).

limited solubility and IC_{50} of these compounds also prevented the detection of *in vivo* activity in *E. coli* swimming motility assays, which only used 0.6% DMSO (Supplementary Fig. S6). Further medicinal chemistry effort should focus on improving both binding affinity and solubility of elaborated compounds. Nevertheless, these results indicate that benzofuran analogues can inhibit DsbA oxidase activity by disrupting the binding of the substrate peptide to the hydrophobic groove of DsbA. It also highlights the significant challenge of developing inhibitors to target a protein site that favours hydrophobic interactions and the importance of evaluating biological activities at the early stage of drug discovery.[27]

3. Conclusions

The dependence of bacterial virulence proteins on DsbA-mediated disulfide bond formation makes this thiol-disulfide oxidoreductase an attractive target for the development of antivirulence therapeutics. For the development of novel inhibitors of *Ec*DsbA, a structure-based ligand design strategy was undertaken starting from 2-(6-bromobenozfuran-3-yl)acetic acid. The fragment hit was first elaborated from the 5- and 6-position using Suzuki-Miyaura coupling to install a small series of phenyl groups. A combination of ligand detected NMR methods and X-ray crystallography identified **2b** as an ideal analogue for further elaboration from C-2 to access a more polar region of the binding groove. X-ray crystal structures of **11**, **13a** and **13b** confirmed C-2 as a valid growth vector to access this region of the binding pocket. Further evaluation by HSQC revealed improved K_D values for C-2 analogues relative to the parent compounds (274 ± 34 μM (**13b**)). Importantly, biochemical assays showed inhibitory activity of C-2 analogues against DsbA and suggest the potential to develop benzofuran analogues into antivirulence compounds.

4. Materials and methods

4.1. General

All commercial materials were used as received without further purification, unless otherwise specified. Purification of solvents and reagents, if required, was carried out by procedures described by Chai and Armarego.[28] Boronic acids were sourced commercially from Advanced Molecular Technology. Moisture sensitive reactions were performed under an atmosphere of nitrogen with all reactions carried out at room temperature, unless otherwise noted. Glassware was oven-dried and cooled under nitrogen prior to use. Analytical Thin Layer Chromatography (TLC) was performed on Merck Kieselgel 60 F254 aluminium backed plates and visualised using a 254 nm UV lamp. Flash chromatography was performed on silica gel (Davisil® LC60Å 40–63 μm). Melting points were determined on a Reichert 'Thermopan' microscope hot stage apparatus and values were corrected by a 12% increase after calibration against known reference samples. Low-resolution electrospray ionisation (ESI) mass spectra were recorded on a Bruker Daltronics Esquire 6000 Ion Trap mass spectrometer in methanol or acetonitrile (0.1% formic acid for positive mode) at 300 °C, a 40 eV cone voltage, with a scan rate of 5500 *m/z/s*. High-resolution electrospray ionisation (ESI) mass spectrometry was carried out using an Agilent Technologies Accurate Mass Q-TOF LC-MS 6530 using Autosampler 1260 Infinity II in positive mode. The samples were analysed using a flow rate of 1 mL/min, a mass range of 100–1000 *m/z* and a scan rate of 10,000 *m/z*/second. Analytical RP-HPLC was performed on a Shimadzu LC-20AB Prominence Liquid Chromatography system fitted with a Phenomenex® Jupiter C18 300 Å column (250 mm × 4.6 mm, 10 μm), using a buffered binary system; solvent A: 0.1% trifluoroacetic acid; solvent B: acetonitrile. Gradient elution was performed using a gradient of 90% solvent A to 90% solvent B over 20 min with a flow rate of 1 mL/min, monitored at 254 nm. Semi-preparative RP-HPLC was performed using a Phenomenex Jupiter C18 column with the same binary buffer system described for RP-HPLC over 60 min with a flow rate of 2 mL/min, unless otherwise stated. The purity of biologically tested compounds was > 95% in all cases, unless specified otherwise. Microwave assisted reactions were performed using a Milestone StartSYNTH system. NMR spectra were recorded on Bruker AV-400 and AV-500 spectrometers at 400.13 and 500.02 MHz respectively, for ^{1}H nuclei and at 100.62 and 125.74 MHz respectively, for ^{13}C nuclei at 300 K. For ^{1}H NMR the residual $CDCl_3$ peak (7.26 ppm) or DMSO-d_6 peak (2.50 ppm) were used as internal standards. Similarly, ^{13}C NMR spectra were referenced to the residual solvent; the central peak of the $CDCl_3$ 'triplet' (77.0 ppm) or DMSO-d_6 'heptet' (40.0 ppm). Chemical shifts were reported as δ values in parts per million (ppm). All coupling constants *J* are measured in Hertz. The following abbreviations have been used for reporting spectral data: s, singlet; d, doublet; dd, doublet of doublets; t, triplet; q, quartet; m, multiplet; and br, broad.

4.2. Chemical syntheses

4.2.1. General procedures

General Procedure A1: Preparation of 5- and 6-aryl analogues *via* Suzuki-Miyaura cross-coupling. A solution of acetonitrile:water (4:1) was degassed by bubbling a stream of nitrogen through the solution for one hour. The aryl halide, boronic acid (6 eq.), caesium fluoride (3 eq.) and $Pd(dppf)Cl_2$ (5 mol%) were added to the degassed solution (25 mL/mmol) and the suspension was heated to 90 °C under an atmosphere of nitrogen. After 16–24 h the reaction mixture was partitioned between ethyl acetate and brine. The organic layer was washed with brine (x2), dried over magnesium sulfate then concentrated to the crude residue. In cases where the aryl halide or boronic acid contained a carboxylic acid the organic phase was washed with a saturated solution of sodium hydrogen carbonate (x3). The combined aqueous phases were acidified with concentrated HCl to pH 2, extracted with ethyl acetate (x3) then worked up as above to afford the crude compound.

General Procedure A2: Microwave assisted Suzuki-Miyaura cross-coupling. Aryl halide (1 eq.), boronic acid (1.2–6 eq.) and caesium fluoride (3 eq.) were dissolved in degassed acetonitrile:water (4:1) (20 mL/mmol) in a Milestone microwave vessel. $Pd(dppf)Cl_2$ was added then the vessel was flushed with nitrogen and quickly sealed. The reaction was irradiated at 90–120 °C for 15–60 min. The reaction was cooled to room temperature then partitioned between ethyl acetate and brine. The organic layer was washed with brine (x2), dried over magnesium sulfate then concentrated under reduce pressure.

General Procedure B: Base mediated ester hydrolysis. Esters were hydrolysed according to the method of Theodorou and co-workers.[29] Esters were dissolved in a mixture of methanol:dichloromethane (1:9) and treated with a 2 M methanolic solution of sodium hydroxide (1–5 eq.) to give a final 0.1 M concentration of ester. The solution was stirred for 3–20 h at which time a cloudy suspension had formed. The suspension was concentrated under reduced pressure and the residue was dissolved in water. The solution was acidified with concentrated HCl to pH 1 then the carboxylic acids were extracted with dichloromethane or ethyl acetate (×3). The combined organic layers were dried over magnesium sulfate then concentrated under reduced pressure. Unless otherwise stated, no purification was required.

4.2.2. 2-(6-(3-Hydroxyphenyl)benzofuran-3-yl)acetic acid (2a)

Compound **1a** (100 mg, 0.392 mmol) was coupled to *m*-hydroxyphenylboronic acid (325 mg, 2.35 mmol) according to General Procedure A1 for 24 h. The crude residue was purified by flash chromatography (20% ethyl acetate, 1% acetic acid in hexanes) to afford the product as a beige solid (55.1 mg, 52%), mp 181–184 °C. δ_H (500 MHz, DMSO-d_6) 9.51 (1H, br s, COOH), 7.89 (1H, s, ArH), 7.73 (1H, s, ArH), 7.63 (1H, d, *J* 8.0, ArH), 7.48 (1H, d, *J* 8.5, ArH), 7.24 (1H, t, *J* 7.8, ArH), 7.12 (1H, d, *J* 7.0, ArH), 7.05 (1H, s, ArH), 7.05 (1H, d, *J* 8.0, ArH), 3.67 (2H, s, CH_2). δ_C (100 MHz, DMSO-d_6) 172.4, 158.3, 155.6, 144.4, 142.2, 137.6, 130.4, 127.6, 122.1, 120.9, 118.2, 114.8, 114.7,

114.3, 109.6, 29.7. LRMS (ESI): *m/z* found 266.9 $(M-H)^-$, HRMS (ESI) did not ionise, $C_{16}H_{11}O_4^-$ required 267.0663.

4.2.3. 2-(6-(3-Methoxyphenyl)benzofuran-3-yl)acetic acid (2b)

Compound **1a** (100 mg, 0.392 mmol) was coupled to *m*-methoxyphenylboronic acid (358 mg, 2.35 mmol) were coupled according to General Procedure A at 90 °C for 24 h. The crude oil was purified by flash chromatography (1–20% ethyl acetate, 1% acetic acid in hexanes) to afford the titled compound as a light brown solid (47.8 mg, 43%), mp 132–133 °C. δ_H (400 MHz, $CDCl_3$) 7.69 (1H, s, ArH), 7.66 (1H, s, ArH), 7.61 (1H, d, *J* 10, ArH), 7.51 (1H, d, *J* 10, ArH), 7.37 (1H, t, *J* 9.8, ArH), 7.21(1H, d, *J* 9.8, ArH), 7.16 (1H, s, ArH), 6.91 (1H, d, *J* 10.5, ArH), 3.88 (3H, s, OCH_3), 3.78 (2H, br s, CH_2). δ_C (100 MHz, $CDCl_3$) 160.0, 155.8, 143.7, 142.7, 138.3, 129.8, 126.8, 122.5, 119.9, 119.7, 113.2, 112.7, 112.4, 110.2, 107.6, 55.3, 29.7. One quaternary carbon not observed. LRMS (ESI): *m/z* found 280.9 $(M-H)^-$. HRMS (ESI): *m/z* found 281.0850 $(M-H)^-$, $C_{17}H_{13}O_4^-$ required 281.0819.

4.2.4. 2-(6-(3-Cyanophenyl)benzofuran-3-yl)acetic acid (2c)

Compound **2b** (300 mg, 0.949 mmol) was coupled to *m*-cyanophenylboronic acid (837 mg, 5.69 mmol) according to General Procedure A1 at 90 °C for 16 h. The crude material was purified by flash chromatography (2.5% methanol in dichloromethane). The fractions containing the product were concentrated under reduced pressure and recrystallised from toluene then from aqueous isopropanol to afford the titled compound as white needles (37.1 mg, 14%), mp 159–161 °C. δ_H (500 MHz, $CDCl_3$) 7.90 (1H, s, ArH), 7.85 (1H, d, *J* 7.9, ArH) 7.71 (1H, s, ArH), 7.68 (1H, s, ArH), 7.66 (1H, d, *J* 8.2, ArH), 7.64 (1H, d, *J* 7.8, ArH), 7.56 (1H, t, *J* 9.7, ArH), 7.47 (1H, d, *J* 8.1, ArH), 3.80 (2H, s, CH_2). δ_C (100 MHz, $CDCl_3$) 175.6, 155.8, 144.2, 142.4, 135.9, 131.7, 130.9, 130.6, 129.7, 127.6, 122.2, 120.3, 118.8, 113.1, 112.4, 110.3, 29.3. LRMS (ESI): *m/z* found 300.1 $(M + Na)^+$. HRMS (ESI): *m/z* found 276.0689 $(M-H)^-$, $C_{17}H_{10}NO_3^-$ required 276.0666.

4.2.5. 2-(5-Phenylbenzofuran-3-yl)acetic acid (2d)

Compound **1c** (100 mg, 0.392 mmol) was coupled to phenylboronic acid (287 mg) according to General Procedure A1 at 90 °C for 16 h. Purification by flash chromatography (20% ethyl acetate, 1% acetic acid in hexanes) gave a crude brown solid. Further purification by semi-preparative RP-HPLC isolated the titled compound as a white solid (5.0 mg, 5%), mp 123–125 °C. δ_H (400 MHz, $CDCl_3$) 7.73 (1H, s, ArH), 7.68 (1H, s, ArH), 7.62–7.59 (2H, m, ArH), 7.54 (2H, d, *J* 1.2, ArH), 7.5 (2H, t, *J* 7.6 ArH), 7.35 (1H, t, ArH), 3.80 (2H, s, CH_2). δ_C (100 MHz, $CDCl_3$) 176.0 (C_q), 154.8 (C_q), 143.7, 141.5 (C_q), 136.6 (C_q), 128.7, 127.9 (C_q),127.5, 127.0, 124.4, 118.1, 112.6 (C_q), 111.7, 29.3 (CH_2). LRMS (ESI): *m/z* found 251.0 $(M-H)^-$. HRMS (ESI): *m/z* found 251.0770 $(M-H)^-$, $C_{16}H_{11}O_3^-$ required 251.0714.

4.2.6. Methyl 2-(6-phenylbenzofuran-3-yl)acetate (4a)

Compound **3a** (200 mg, 0.743 mmol) was coupled to phenylboronic acid (136 mg, 1.12 mmol) according to General Procedure A1 at 60 °C for 28 h. The crude compound was purified by flash chromatography (1–10% ethyl acetate in hexanes) which isolated the starting material along with the cross-coupled compound. The two compounds were separated by semi-preparatory RP-HPLC to afford the titled compound as a white powder (40 mg, 20%), mp 106–108 °C. δ_H (500 MHz, $CDCl_3$) 7.70 (1H, s, ArH), 7.66 (1H, s, ArH), 7.65–7.61 (3H, m, ArH), 7.25 (1H, dd, *J* 8.5, 1.5, ArH), 7.47–7.44 (2H, m, ArH), 7.36 (1H, t, *J* 5.5, ArH), 3.75 (3H, s, OCH_3), 3.74 (2H, s, CH_2). δ_C (125 MHz, $CDCl_3$) 171.1 (C_q), 155.9 (C_q), 143.4, 141.2 (C_q), 138.3 (C_q), 128.8, 127.4, 127.2, 126.8 (C_q), 122.3, 119.8, 113.0 (C_q), 110.1, 52.2 (OCH_3), 29.6 (CH_2). LRMS (ESI): *m/z* found 267.1 $(M+H)^+$, $C_{17}H_{15}O_3^+$ required 267.1.

4.2.7. Methyl 2-(6-(4-methoxyphenyl)benzofuran-3-yl)acetate (4c)

Compound **3b** (100 mg, 317 μmol) was coupled to *p*-methoxyphenylboronic acid (1.90 mmol) according to General Procedure A2 at 80 °C for one hour. The crude brown solid was purified by flash chromatography (2.5% ethyl acetate in hexanes) to afford the titled compound as an off white solid (60.9 mg, 65%), mp 154–156 °C. δ_H (500 MHz, $CDCl_3$) 7.65 (1H, s, ArH), 7.64 (1H, s, ArH), 7.59 (1H, d, *J* 8.1, ArH), 7.57 (2H, d, *J* 8.9, ArH), 7.47 (1H, d, *J* 8.1, ArH), 7.00 (2H, d, *J* 8.9, ArH), 3.86 (3H, s, OCH_3), 3.75 (3H, s, OCH_3), 3.73 (2H, s, CH_2). δ_C (125 MHz, $CDCl_3$) 171.1, 159.1, 155.9, 143.1, 138.0, 133.8, 128.4, 126.3, 122.0, 119.7, 114.3, 113.0, 109.6, 55.3, 52.1, 29.6. LRMS (ESI): *m/z* found 297.2 $(M+H)^+$, $C_{18}H_{17}O_4^+$ required 297.1121.

4.2.8. Methyl 2-(6-(3-(trifluoromethyl)phenyl)benzofuran-3-yl)acetate (4d)

Compound **3b** (200 mg, 0.633 mmol) was coupled to *m*-fluorophenylboronic acid (132 mg) according to General Procedure A2 at 120 °C for 15 min. The crude brown oil was purified by flash chromatography (2.5–5% ethyl acetate in hexanes) which afforded the titled compound as a white solid (153 mg, 72%), mp 75–77 °C. δ_H (500 MHz, $CDCl_3$) 7.88 (1H, s, ArH), 7.80 (1H, d, *J* 7.6, ArH), 7.70 (1H, s, ArH), 7.69 (1H, s, ArH), 7.65 (1H, d, *J* 8.1, ArH), 6.61 (1H, d, *J* 7.8, ArH), 7.57 (1H, t, *J* 7.7, ArH), 7.51 (1H, d, *J* 8.1, ArH), 3.76 (3H, s, OCH_3), 3.75 (2H, s, CH_2). δ_C (125 MHz, $CDCl_3$) 171.0 (C_q), 155.8 (C_q), 143.8, 142.0, 136.7, 131.2 (C_q, q, *J* 32.0), 130.6, 129.3, 127.5 (C_q), 124.2 (C_q, d, *J* 272.4), 124.1 (q, *J* 3.8), 123.8 (q, *J* 3.7), 122.2, 120.1, 113.1 (C_q), 110.2, 52.2 (OCH_3), 29.5 (CH_2). δ_F (376 MHz, $CDCl_3$) −62.6. LRMS (ESI): *m/z* found 335.2 $(M+H)^+$, $C_{18}H_{14}F_3O_3^+$ required 335.1.

4.2.9. 2-(6-Phenylbenzofuran-3-yl)acetic acid (5a)

Ester **4a** (20.0 mg, 75.1 μM) was hydrolysed using 2 M methanolic sodium hydroxide (1.5 eq, 57.8 μL) according to General Procedure B. The resulting suspension was worked up after 20 h to afford the titled product as a white solid (13.2 mg, 80%), mp 166–167 °C. δ_H (500 MHz, $CDCl_3$) 7.70 (1H, s, ArH), 7.68 (1H, s, ArH), 7.64–7.62 (3H, m, ArH), 7.52 (1H, dd, *J* 8.0, 1.5, ArH), 7.47–7.44 (2H, m, ArH), 7.36 (1H, t, *J* 7.5, ArH), 3.79 (1H, s, CH_2). δ_C (100 MHz, $CDCl_3$) 175.7 (C_q), 155.9 (C_q), 143.6, 141.2 (C_q), 138.5 (C_q), 128.8, 127.4, 127.2, 126.6 (C_q), 122.4, 199.7, 112.4 (C_q), 110.1, 29.4 (CH_2). LRMS (ESI): *m/z* found 250.9 $(M-H)^-$. HRMS (ESI): *m/z* found 251.0732 $(M-H)^-$, $C_{16}H_{11}O_3^-$ required 251.0714.

4.2.10. 2-(6-(3-Carboxyphenyl)benzofuran-3-yl)acetic acid (5b)

Compound **3a** (200 mg, 0.743 mmol) was coupled to *m*-carboxyphenylboronic (185 mg, 1.11 mmol) as per General Procedure A1 at 90 °C for 24 h. Flash chromatography (1.25% methanol in dichloromethane) isolated a mixture of the coupled product and an inseparable by-product in a 1:1 ratio. Semi-preparative RP-HPLC improved the ratio of cross-coupled product and a by-product to a ratio of 2:1. The mixture was hydrolysed according to General Procedure B to give the crude acid. Purification by flash chromatography (1.25–2.5% methanol, 1% acetic acid in dichloromethane) afforded the titled compound as a white solid (30 mg, 14%), mp 129–132 °C. δ_H (400 MHz, DMSO-d_6) 8.22 (1H, s, ArH), 7.98–7.89 (4H, m, ArH), 7.69 (1H, d, *J* 8.0, ArH), 7.61–7.57 (2H, m, ArH), 3.72 (2H, s, CH_2). δ_C (100 MHz, DMSO-d_6) 172.4 (C_q), 167.8 (C_q), 155.8 (C_q), 144.9, 141.11 (C_q), 136.5 (C_q), 132.0 (C_q), 132.0, 129.9, 128.6, 128.1 (C_q), 128.0, 122.3, 121.3, 114.6 (C_q), 110.1, 29.5 (CH_2). LRMS (ESI): *m/z* found 295.3 $(M-H)^-$. HRMS *m/z* found 295.0643 $(M-H)^-$, $C_{17}H_{11}O_5^-$ required 295.0612.

4.2.11. 2-(6-(4-Methoxyphenyl)benzofuran-3-yl)acetic acid (5c)

Ester **4c** (57.4 mg, 194 μmol) was hydrolysed using 2 M methanolic sodium hydroxide (3 eq., 29.1 μL) according to General Procedure B. The resulting turbid solution was worked up after 16 h to afford the titled compound as an off white solid (49.2 mg, 90%), mp 220–222 °C. δ_H (400 MHz, DMSO-d_6) 7.90 (1H, s, ArH), 7.79 (1H, s, ArH), 7.68–7.62 (3H, m, ArH), 7.53 (1H, d, *J* 8.2, ArH), 7.03 (2H, d, *J* 8.7, ArH), 3.80 (3H, s, OCH_3), 3.71 (2H, s, CH_2). δ_C (100 MHz, DMSO-d_6) 172.4, 159.3, 155.8, 144.2, 137.2, 133.1, 128.5, 127.0, 121.8, 120.9, 114.9, 114.5,

109.2, 55.7, 29.5. LRMS (ESI): *m/z* found 280.93 $(M-H)^-$. HRMS (ESI): *m/z* found 281.0846 $(M-H)^-$, $C_{17}H_{13}O_4^-$ required 281.0819.

4.2.12. 2-(6-(3-(Trifluoromethyl)phenyl)benzofuran-3-yl)acetic acid (5d)

Ester **4d** (152 mg, 0.455 mmol) was hydrolysed using 2 M methanolic sodium hydroxide (3 eq., 682 μL) according General Procedure B to afford the titled compound as a white solid (132 mg, 91%), mp 123–125 °C. δ_H (400 MHz, $CDCl_3$) 7.87 (1H, s, ArH), 7.80 (1H, d, *J* 7.5, ArH), 7.71 (1H, s, ArH), 7.69 (1H, s, ArH), 7.65 (1H, d, *J* 8.1, ArH), 7.61 (1H, d, *J* 7.9, ArH), 7.57 (1H, t, *J* 7.6, ArH), 7.51 (1H, d, *J* 8.1, ArH), 3.80 (2H, s, CH_2). δ_C (100 MHz, $CDCl_3$) 176.6 (C_q), 155.8 (C_q), 144.0, 141.9 (C_q), 136.8 (C_q), 131.2 (C_q, q, *J* 32.0), 130.6, 129.3, 127.3, 124.2 (C_q, d, *J* 270.4), 124.1 (q, 3.7), 123.9 (q, *J* 3.7), 122.3, 120.1, 112.3 (C_q), 110.3, 29.4 (CH_2). δ_F (376 MHz, $CDCl_3$) −63.6. LRMS (ESI): *m/z* found 318.9 $(M-H)^-$. HRMS (ESI): *m/z* found 319.0617 $(M-H)^-$, $C_{17}H_{10}F_3O_3^-$ required 319.0588.

4.2.13. Methyl 2-(2,6-dimbromobenzofuran-3-yl)acetate (6a)

A solution of **3a** (100 mg, 0.371 mmol) in acetic acid (3.23 mL) was treated with a solution of bromine (19.0 μL) in acetic acid (808 μL) and the brown solution stirred at room temperature for 3 h. The solution was poured onto cracked ice and the solid that precipitated was collected by vacuum filtration. The crude off white solid was recrystallised from isopropanol to afford the titled compound as a white solid (67.2 mg, 52%), mp 120–122 °C. δ_H (500 MHz, $CDCl_3$) 7.62 (1H, s, ArH), 7.39 (1H, d, *J* 8.0, ArH), 7.37 (1H, d, *J* 8.5, ArH), 3.72 (3H, s, OCH_3), 3.65 (2H, s, CH_2). δ_C (125 MHz, $CDCl_3$) 175.2 (C_q), 155.5 (C_q), 132.5, 129.2 (C_q), 127.6 (C_q), 120.5, 120.3, 112.5 (C_q), 88.2 (C_q), 30.0, 25.2. LRMS (ESI): *m/z* found 368.52 $(M[^{79}Br,^{79}Br] + Na)^+$, 370.93 $(M[^{79}Br,^{81}Br] + Na)^+$, 372.92 $(M[^{81}Br,^{81}Br] + Na)^+$. HRMS (ESI): *m/z* found 368.8744 $(M[^{79}Br,^{79}Br] + Na)^+$, 370.8725 $(M[^{79}Br,^{81}Br] + Na)^+$, 372.8700 $(M[^{81}Br,^{81}Br] + Na)^+$, $C_{11}H_8[^{79,79}Br]_2NaO_3^+$ required 368.8732, $C_{11}H_8[^{79,81}Br]_2NaO_3^+$ required 370.8712, $C_{11}H_8[^{81,81}Br]_2NaO_3^+$ required 372.8691.

4.2.14. Suzuki coupling of 6a to phenylboronic acid to give 7a-c

Dibromo **6a** (43 mg, 0.1224 mmol) was coupled to phenylboronic acid according to General Procedure A1 at 90 °C for 24 h, after which time analytical RP-HPLC indicated unreacted starting material and three new products. The reaction mixture was cooled to room temperature and treated with brine then extracted with ethyl acetate (x3). The combined organic phase was dried ($MgSO_4$) then concentrated under reduced pressure to a brown residue. The crude material, which comprised of starting material and three products, was separated by semi-preparative RP-HPLC. The fractions containing **6a** and **7a-c** were lyophilised. Unreacted starting material **6a** eluted at 19.7 min (10 mg, 23% recovery). *Methyl 2-(2-bromo-6-phenylbenzofuran-3-yl)acetate* (**7a**) eluted at 21.2 min (2.0 mg, 1%). δ_H (500 MHz, $CDCl_3$) 7.65 (1H, dd, *J* 1.4, 0.6, ArH), 7.62–7.61 (1H, m, ArH), 6.61–7.60 (1H, m, ArH), 7.55 (1H, dd, *J* 8.13, 0.6, ArH), 7.51 (1H, dd, *J* 8.2, 1.5, ArH), 7.46 (2H, m, ArH), 7.36 (1H, tt, 7.4, 1.2, ArH), 3.74 (3H, s, OCH_3), 3.70 (2H, s, CH_2). *Methyl 2-(6-bromo-2-phenylbenzofuran-3-yl)acetate (7b)* eluted at 22.1 min (6.4 mg, 15%). δ_H (500 MHz, $CDCl_3$) 7.82–7.80 (2H, m, ArH), 7.68 (1H, dd, *J* 1.6, 0.4, ArH), 7.52–7.49 (2H, m, ArH), 7.48 (1H, dd, *J* 8.4, 0.35, ArH), 7.43 (1H, tt, *J* 7.4, 1.29, ArH), 7.40 (1H, dd, *J* 8.29, 1.65, ArH), 3.86 (2H, s, CH_2), 3.75 (3H, s, OCH_3). Regioisomers **7a** and **7b** were distinguishable from on another due to the chemical shift of the methylene singlet (see supplementary Fig. S5). *Methyl 2-(2,6-diphenylbenzofuran-3-yl)acetate (7c)* eluted at 23.1 min (2.6 mg, 1%). δ_H (500 MHz, $CDCl_3$) 7.87–7.85 (2H, m, ArH), 7.74 (1H, d, *J* 0.9, ArH), 7.68–7.65 (3H, m, ArH), 7.55–7.50 (3H, m, ArH), 7.49–7.45 (2H, m, ArH), 7.43 (1H, tt, *J* 7.4, 1.2, ArH), 7.36 (1H, tt, *J* 7.3, 1.2, ArH), 3.92 (2H, s, CH_2), 3.77 (3H, s, OCH_3).

4.2.15. 2-(6-Bromo-2-phenylbenzofuran-3-yl)acetic acid (8a)

Compound **7b** (6.4 mg, 0.019 mmol) was hydrolysed using 2 M methanolic sodium hydroxide (3 eq., 46 μL) according to General Procedure B to afford the titled compound as a white solid (6.1 mg, 100%). δ_H (400 MHz, $CDCl_3$) 7.79 (2H, s, ArH), 7.68 (1H, s, ArH), 7.52–7.38 (5H, m, ArH), 3.88 (2H, s, CH_2), 2.17 (3H, s, OCH_3). δ_C (100 MHz, $CDCl_3$) 175.8 (C_q), 154.2 (C_q), 153.8 (C_q), 129.7 (C_q), 129.2, 128.9, 128.8, 127.4, 126.3, 129.7, 118.0 (C_q), 114.7, 107.9 (C_q), 30.91 (CH_2).

4.2.16. 2-(2,6-Diphenylbenzofuran-3-yl)acetic acid (8b)

Compound **7c** (2.6 mg, 0.0076 mmol) was hydrolysed using 2 M methanolic sodium hydroxide (5 eq., 16 μL) according General Procedure B to afford the titled compound as a white solid (2.5 mg, 100%). δ_H (400 MHz, $CDCl_3$) 7.84 (2H, d, *J* 1.4, ArH), 7.74 (1H, s, ArH), 7.68–7.64 (3H, m, ArH), 7.55–7.41 (6H, m, ArH), 7.36 (1H, t, *J* 7.4, ArH), 3.95 (2H, s, CH_2). δ_C (100 MHz, $CDCl_3$) 175.3 (C_q), 154.6 (C_q), 153.7 (C_q), 141.3 (C_q), 138.6 (C_q), 130.2 (C_q), 128.93, 128.91, 128.88, 128.84, 127.40, 127.39, 127.2, 122.6 (C_q), 199.8, 109.7, 107.9 (C_q), 53.4, 29.7 (CH_2).

4.2.17. Methyl 2-(2-bromo-6-iodobenzofuran-3-yl)acetate (9a)

Compound **3b** (1.06 g, 3.35 mmol) was dissolved in acetic acid (20 mL) and treated with bromine (189 μL, 3.68 mmol). The reaction stirred for three hours then was poured onto ice. The resulting precipitate was collected by vacuum filtration then recrystallised from isopropanol to give the titled compound as an off white solid (751 mg, 57%), mp 131–133 °C. δ_H (400 MHz, $CDCl_3$) 7.80 (1H, s, ArH), 7.56 (1H, d *J, J* 8.2, ArH), 7.25 (1H, d *J, J* 8.3, ArH), 3.72 (3H, s, OCH_3), 3.64 (2H, s, CH_2). δ_C (100 MHz, $CDCl_3$) 169.8 (C_q), 155.5 (C_q), 132.5, 128.8 (C_q), 127.8 (C_q), 120.6, 120.2, 113.1 (C_q), 88.0 (C_q), 52.3 (OCH_3), 30.2 (CH_2). LRMS (ESI): *m/z* found 394.92 $(M[^{79}Br] + H)^+$, 396.92 $(M[^{81}Br] + H)^+$. HRMS *m/z* found 394.8798 $(M[^{79}Br] + H)^+$, 396.8760 $(M[^{81}Br] + H)^+$, $C_{11}H_9[^{79}Br]IO_3^+$ required 394.8774, $C_{11}H_9[^{81}Br]IO_3^+$ required 396.8754.

4.2.18. Methyl 2-(2-bromo-6-(3-methoxyphenyl)benzofuran-3-yl)acetate (10a)

Compound **9a** (600 mg, 0.506 mmol) was coupled to *m*-methoxyphenylboronic acid (254 mg) according to General Procedure A2 at 80 °C for 1 h. Purification by flash chromatography (2.5% ethyl acetate in hexanes) afforded the titled compound as an oily light brown semi solid which was lyophilised to a white powder (315 mg, 55%), mp 50–52 °C. δ_H (500 MHz, $CDCl_3$) 7.65 (1H, s, ArH). 7.55 (1H, d, *J* 8.2, ArH), 7.50 (1H, d, *J* 8.2, ArH), 7.37 (1H, t, *J* 8.0, ArH), 7.20 (1H, d, *J* 7.7, ArH), 7.14 (1H, s, ArH), 7.92 (1H, d, *J* 8.2, ArH), 6.90 (3H, s, OCH_3), 3.74 (3H, s, OCH_3), 3.70 (2H, s, CH_2). δ_C (100 MHz, $CDCl_3$) 170.1, 160.0, 155.8, 142.4, 138.2, 129.9, 128.6, 127.4, 123.0, 119.8, 119.2, 113.1, 113.0, 112.7, 109.6, 55.3, 52.3, 30.3. LRMS (ESI): *m/z* found 375.1 $(M[^{79}Br] + H)^+$, 377.0 $(M[^{81}Br] + H)^+$, $C_{18}H_{16}[^{79}Br]O_4^+$ required 375.0, $C_{18}H_{16}[^{81}Br]O_4^+$ required 377.0.

4.2.19. Methyl 2-(2,6-bis(3-methoxyphenyl)benzofuran-3-yl)acetate (10b)

Compound **9a** (100 mg, 0.253 mmol) was coupled to *m*-methoxyphenylboronic acid (156 mg) according to General Procedure A2 at 80 °C for 50 min. Purification by flash chromatography (5–10% ethyl acetate in hexanes) afforded the titled compound as a light brown oil (77.6 mg, 76%), mp 91–91 °C. δ_H (400 MHz, $CDCl_3$) 7.73 (1H, s, ArH), 6.67 (1H, d, *J* 8.1, ArH), 7.54 (1H, d, *J* 8.1, ArH), 7.45–7.37 (4H, m, ArH), 7.26–7.24 (1H, m, ArH), 7.20 (1H, s, ArH), 7.00–6.97 (1H, m, ArH), 6.92 (1H, d, *J* 8.2), 3.92 (2H, s, CH_2), 3.91 (3H, s, OCH_3), 3.76 (3H, s, OCH_3). δ_C (100 MHz, $CDCl_3$) 171.3, 156.0, 159.9, 154.5, 153.4, 142.8, 138.3, 131.5, 129.9, 129.8, 129.2, 122.5, 119.9, 119.8, 119.8, 115.1, 113.1, 112.6, 112.4, 109.7, 108.8, 55.4, 55.3, 52.3, 30.7. LRMS (ESI): *m/z* found 425.1 $(M + Na)^+$, $C_{25}H_{22}NaO_5^+$ required 425.1.

4.2.20. 2-(2,6-Bis(3-methoxyphenyl)benzofuran-3-yl)acetic acid (11)

Ester **10b** (77.0 mg, 0.191 mmol) was hydrolysed using 2 M

methanolic sodium hydroxide (3 eq., 287 μL) according to General Procedure B. Purification by flash chromatography (5% methanol in dichloromethane) afforded the titled compound as an off-white semi-solid (40.4 mg, 54%), 137–139 °C. δ_H (500 MHz, $CDCl_3$) 7.73 (1H, s, ArH), 7.66 (1H, d, *J* 8.1, ArH), 7.53 (1H, d, *J* 8.1, ArH), 7.42–7.41 (3H, m, ArH), 7.38 (1H, t, *J* 7.9, ArH), 7.25 (1H, d, *J* 7.6, ArH), 7.19 (1H, s, ArH), 7.00–6.96 (1H, m, ArH), 6.92 (1H, d, *J* 8.2, ArH), 3.94 (2H, s, CH_2), 3.89 (6H, s, OCH_3). δ_C (125 MHz, $CDCl_3$) 176.8 (C_q), 160.0 (C_q), 159.9 (C_q), 154.4 (C_q), 153.6 (C_q), 142.8 (C_q), 138.4 (C_q), 131.3 (C_q), 129.9, 129.8, 129.0, 122.6, 119.9, 119.8, 119.8, 115.1, 113.1, 1126, 112.5, 109.8, 108.1 (C_q), 55.4 (OCH_3), 55.3 (OCH_3), 30.6 (CH_2). LRMS (ESI): *m/z* found 389.2 $(M+H)^+$. HRMS (ESI) did not ionise, $C_{24}H_{21}O_5^+$ required 389.1.

4.2.21. Methyl 2-(6-(3-methoxyphenyl)-2-(4-methoxyphenyl)benzofuran-3-yl)acetate (12a)

Compound **10a** (94.0 mg, 0.251 mmol) was coupled to *m*-methoxyphenylboronic acid (76.1 mg) according to General Procedure A2 at 80 °C for 50 min. Purification by flash chromatography (5–10% ethyl acetate in hexanes) afforded the titled compound as an oily light brown semi-solid which was lyophilised to an off-white solid (60.8 mg, 60%), mp 109–111 °C. δ_H (400 MHz, $CDCl_3$) 7.81 (2H, d, *J* 9.0, ArH), 7.72 (1H, s, ArH), 7.64 (1H, d, *J* 8.1, ArH), 7.52 (1H, d, *J* 8.1, ArH), 7.38 (1H, t, *J* 7.9, ArH), 7.26–7.24 (1H, m, ArH), 7.20 (1H, s, ArH), 7.05 (2H, d, *J* 8.9, ArH), 6.91 (1H, d, *J* 8.2, ArH), 3.89 (3H, s, OCH_3), 3.88 (3H, s, OCH_3), 3.88 (2H, s, CH_2), 3.76 (3H, s, OCH_3). δ_C (100 MHz, $CDCl_3$) 171.4, 160.1, 160.0, 154.3, 153.6, 142.9, 137.8, 129.8, 129.4, 128.8, 122.9, 122.4, 119.8, 119.5, 114.3, 113.1, 112.5, 109.5, 107.2, 55.3, 55.3, 52.3, 30.6. LRMS (ESI): *m/z* found 403.2 $(M+H)^+$, $C_{25}H_{23}O_5^+$ required 403.2.

4.2.22. 3-(3-(2-Methoxy-2-oxoethyl)-6-(3-methoxyphenyl)benzofuran-2-yl)benzoic acid (12b)

Compound **10a** (44 mg, 0.267 mmol) was coupled to *m*-carboxyphenylboronic acid (66.3 mg) according to General Procedure A2 at 120 °C for 15 min. Purification by flash chromatography (2.5% methanol in dichloromethane) afforded the titled compound as an off-white solid (87.4 mg, 79%), mp 60–62 °C. δ_H (400 MHz, $CDCl_3$) 8.65 (1H, s, ArH), 8.18 (1H, d, *J* 7.8, ArH), 8.13 (1H, d, *J* 7.8, ArH), 7.76 (1H, s, ArH), 7.69 (1H, d, *J* 8.1, ArH), 7.65 (1H, t, *J* 7.8, ArH), 7.56 (1H, d, *J* 8.1, ArH), 7.39 (1H, t, *J* 7.9, ArH), 7.26 (1H, d, *J* 7.6, ArH), 7.20 (1H, s, ArH), 6.93 (1H, d, *J* 8.2, ArH), 3.95 (2H, s, CH_2), 3.90 (3H, s, OCH_3), 3.80 (3H, s, OCH_3). δ_C (100 MHz, $CDCl_3$) 171.4 (C_q), 171.0 (C_q), 160.0 (C_q), 154.6 (C_q), 152.0 (C_q), 142.7 (C_q), 138.7 (C_q), 132.2, 130.9 (C_q), 130.2, 130.0 (C_q), 129.8, 129.1, 129.0 (C_q), 128.9, 122.8, 120.0, 119.9, 113.1, 112.7, 109.8, 109.6 (C_q), 55.3 (OCH_3), 52.4 (OCH_3), 30.6 (CH_2). LRMS (ESI): *m/z* found 417.1 $(M+H)^+$, $C_{25}H_{21}O_6^+$ required 417.1.

4.2.23. 2-(6-(3-Methoxyphenyl)-2-(4-methoxyphenyl)benzofuran-3-yl) acetic acid (13a)

Compound **12a** (60 mg, 0.149 mmol) was hydrolysed using 2 M methanolic sodium hydroxide (3 eq., 224. μL) according to General Procedure B. The titled compound was afforded as a pale brown oil that solidified under reduced pressure to a light brown solid (30.4 mg, 53%), mp 150–153 °C. δ_H (500 MHz, $CDCl_3$) 7.79 (2H, d, *J* 8.9, ArH), 7.71 (1H, s, ArH), 7.64 (1H, d, *J* 8.1, ArH), 7.52 (1H, d, *J* 8.1, ArH), 7.38 (1H, t, *J* 7.9, ArH), 7.24 (1H, d, *J* 7.6, ArH), 7.19 (1H, s, ArH), 7.04 (2H, d, *J* 8.9, ArH), 6.91 (1H, d, *J* 8.2, ArH), 3.90 (2H, s, CH_2), 3.89 (3H, s, OCH_3), 3.87 (3H, s, OCH_3). δ_C (125 MHz, $CDCl_3$) 199.1 (C_q), 160.2 (C_q), 160.0 (C_q), 154.3 (C_q), 153.9 (C_q), 142.9 (C_q), 137.9 (C_q), 129.8, 129.2 (C_q), 128.8, 122.7 (C_q), 122.5, 119.9, 119.5, 114.3, 113.1, 112.6, 109.6, 106.5 (C_q), 55.4 (OCH_3), 55.3 (OCH_3), 30.5 (CH_2). LRMS (ESI): *m/z* found 411.1 $(M + Na)^+$. HRMS (ESI) did not ionise, $C_{24}H_{20}NaO_5^+$ required 411.1.

4.2.24. 3-(3-(Carboxymethyl)-6-(3-methoxyphenyl)benzofuran-2-yl) benzoic acid (13b)

Ester **12b** (87.2 mg, 0.209 mmol) was hydrolysed using 2 M methanolic sodium hydroxide (5 eq., 524 μL) according to General Procedure B. The reaction was worked up after 16 h to afford the titled compound as a white solid (76.6 mg, 91%), mp 244–246 °C. δ_H (400 MHz, DMSO-d_6) 8.39 (1H, s, ArH), 8.06 (1H, d, *J* 7.7, ArH), 8.01 (1H, d, *J* 8.0, ArH), 7.99 (1H, s, ArH), 7.75 (1H, d, J, 8.3, ArH), 7.70 (1H, t, *J* 7.8, ArH), 7.65 (1H, d, *J* 8.2, ArH), 7.39 (1H, t, *J* 7.8, ArH), 7.32 (1H, d, *J* 7.7, ArH), 7.29 (1H, s, ArH), 6.94 (1H, d, *J* 7.9, ArH), 3.94 (2H, s, CH_2), 3.84 (3H, s, OCH_3). δ_C (100 MHz, DMSO-d_6) 172.1 (C_q), 167.3 (C_q), 160.3 (C_q), 154.4 (C_q), 151.6 (C_q), 142.1 (C_q), 138.1 (C_q), 132.1 (C_q), 131.0, 130.7 (C_q), 130.5, 130.0, 129.9, 129.7 (C_q), 127.7 122.8, 121.0, 119.8, 113.6, 112.9, 111.3 (C_q), 109.7, 55.6 (OCH_3), 30.5 (CH_2). LRMS (ESI): *m/z* found 400.9 $(M-H)^-$. HRMS (ESI): *m/z* found 401.1077 $(M-H)^-$, $C_{24}H_{17}O_6^-$ required 401.1031.

4.3. Expression and Purification of Unlabelled and ^{15}N-Labelled *Ec*DsbA

Unlabelled and ^{15}N-labelled *Ec*DsbA were prepared as previously described.[14] Briefly, both unlabelled and ^{15}N-labelled *Ec*DsbA were expressed by autoinduction using appropriate media. After harvesting the cells, periplasmic proteins were extracted by resuspending cell pellet with lysis buffer (20 mM Tris-HCl, pH 8.0, 25 mM NaCl, 4 mg/mL colistin sulfate) and incubating for 18–24 h with gentle stirring at 4 °C. After centrifugation, *Ec*DsbA was purified from the supernatant using a three-step purification method, including hydrophobic interaction chromatography, anion exchange chromatography, and size exclusion chromatography. DsbA was oxidised with copper-phenanthroline and buffer exchanged to the final storage buffer (20 mM HEPES, pH 7.0).

4.4. Protein crystallisation and structure determination

*Ec*DsbA was crystallised as previously described.[14] Briefly, 1 μL of 30 mg/mL *Ec*DsbA was mixed with an equal volume of crystallisation buffer (11–13% PEG8000, 5–7.5% glycerol, 1 mM $CuCl_2$, 100 mM, sodium cacodylate pH 6.1) and equilibrated against 500 μL of reservoir buffer at 20 °C using hanging drop vapour diffusion. For compound soaking, crystals were transferred into 2 μL drops of 24% PEG8000, 22% glycerol, and 100 mM sodium cacodylate (pH 6.1) containing a compound of interest at the final concentration of 10 mM (5% DMSO) and were incubated for 3–6 h. Crystals were mounted on loops and flash-cooled in liquid nitrogen.

Datasets were collected at the Australian synchrotron on MX1 and MX2 beamlines using the Blue-Ice software (CA, USA).[30] MX1 beamline was equipped with an ADSC Quantum 210r detector and MX2 with an ADSC Quantum 315r detector. All datasets were indexed and integrated with iMOSFLM[31] or XDS[32] and scaled using AIMLESS.[33,34] Phasing was performed by molecular replacement with Phaser[35] using the previously solved structure of *Ec*DsbA as a search model (PDB code 1FVK).[36] The final structure was obtained after several rounds of manual model building using Coot[37] and refinement in phenix.refine.[38] Data collection and refinement statistics are summarised in Table S1. Structures, factors and coordinates have been deposited in the Protein Data Bank (PDB; http://www.pdb.org) under the accession codes of 7L76, 7L7C, 7LHP, 6XSP, 6XSQ and 6XT3.

4.5. NMR spectroscopy

For ligand-detected NMR spectroscopy, two samples (compound alone and compound + protein) were prepared for each compound. Unlabelled *Ec*DsbA was prepared at 10 μM in a buffer of 50 mM sodium phosphate, pH 6.8, 25 mM NaCl, 100 μM 4,4-dimethyl 4-silapentane-1-sulfonic acid (DSS), and 10% ^2H_2O. Compound was added to the protein sample to achieve final concentration of 500 μM (2% $^2H_6$-DMSO). ^{1}H 1D spectrum was acquired for each compound at 500 μM as a reference

spectrum. All ligand-detected NMR experiments (STD, CPMG, and waterLOGSY) were acquired at 298 K on a Bruker Avance III 600 MHz NMR spectrometer equipped with a 5 mm TXI CryoProbe. STD spectra were acquired with 3 s of saturation at −1 ppm (on-resonance) and 33.3 ppm (off-resonance). Compounds that gave an average difference in signal intensity > 3% between the on- and off-resonance were identified as hits. WaterLOGSY spectra were acquired for compound alone and compound + protein with a 0.52 s acquisition time, 3 s relaxation delay, and 3 s NOE (Nuclear Overhauser Effect) mixing time. Compounds that gave an average difference in signal intensity > 70% between compound alone and compound + protein were identified as hits. CPMG spectra for compound alone and compound + protein were acquired with a constant spin echo delay of 1 ms and spin-lock period of 350 ms. Compounds that gave an average difference in signal intensity > 30% between compound alone and compound + protein were identified as hits. The data was analysed using Topspin3.5 (Bruker) and DSS was used to reference the spectra.

For the 2D ^{1}H-^{15}N-HSQC titration experiment, 100 μM of ^{15}N-labelled *Ec*DsbA in a buffer of 50 mM HEPES, pH 6.8, 50 mM NaCl, 2% $^{2}H_6$-DMSO, and 10% $^{2}H_2O$, was titrated with increasing concentrations of compounds (0, 0.625, 0.125, 0.25, 0.5, and 1 mM). Data were acquired on a Bruker 600 MHz spectrometer equipped with a 5 mm TXI CryoProbe and a Bruker 700 MHz spectrometer equipped with a 5 mm TXI CryoProbe. Data was processed by Topspin3.5 (Bruker) and analysed by Sparky (T. D. Goddard and D. G. Kneller, SPARKY 3, University of California, San Francisco (UCSF)). Weighted chemical shift perturbations (CSP) that were observed upon addition of compounds to *Ec*DsbA were calculated using equation 1 [39]:

$$CSP = \sqrt{\Delta\delta_H{}^2 + (0.2 \times \Delta\delta_N)^2},$$

where $\Delta\delta_H$ and $\Delta\delta_N$ denote the change in chemical shift of amide proton and nitrogen resonances upon addition of the compound. Equilibrium dissociation constants (K_D) were determined by fitting the plot of CSP against compound concentrations using one site with ligand depletion model (equation 2):

$$CSP = \frac{CSP_{max} \times \left[(K_D + P_t + L_t) - \sqrt{\left((K_D + P_t + L_t)^2 - 4 \times P_t \times L_t\right)} \right]}{2 \times P_t},$$

where CSP is the measured CSP at a given concentration, CSP_{max} is the CSP observed at the saturating concentration of compound, and P_t and L_t are the total protein and compound concentrations. The ligand efficiency (LE) is calculated using equation 3 [40]:

$$LE = -\frac{\Delta G}{HAC} = -\frac{RTln(K_D)}{HAC}$$

where R is gas constant (1.9858775 cal K^{-1} mol^{-1}), T is temperature (298 K), K_D is equilibrium dissociation constant, and HAC is the number of heavy (non-hydrogen) atoms.

4.6. Peptide oxidation assay

The ability of compounds to inhibit the activity of *Ec*DsbA was evaluated using a peptide oxidation assay as previously described.[40] Inhibition of DsbA activity is assessed as a reduction in the rate of fluorescence signal increase in the presence of compounds. A standard 50 μL reaction mixture consists of 0.5 μM *Ec*DsbA, 1 mM oxidised glutathione, 16 μM substrate peptide (DOTA/Eu(III)-CQQGFDGTQNSCK-MCA) and compounds in a buffer of 50 mM MES, pH 5.5, 50 mM NaCl, 2 mM EDTA, 2% DMSO. Assays were performed in a PerkinElmer 384-well white opaque microplate (OptiPlate-384). The time-resolved fluorescence of substrate peptide oxidation (excitation λ = 340 nm and emission λ = 615 nm) was measured using a CLARIOstar plate reader (BMG Labtech) fitted with TR-FRET module. Data was analysed and plotted using GraphPad Prism 8.

4.7. Motility assays

Swimming motility of *E. coli* JCB816 was assessed as previously described.[41] Briefly, 2 μL of four independent liquid overnight JCB816 cultures were inoculated onto the surface of LB semi-solid (0.3% w/v) agar containing 0.6% dimethyl sulfoxide (DMSO) or DsbA inhibitors **11**, **13a** or **13b** at various concentrations (5 μM – 1 mM). Plates were incubated at 37 °C, and the diameter of bacterial outward growth was measured in millimetres at 6 and 9 h post inoculation. The mean motility zone diameter was calculated from four replicates tested under each condition, and group means were compared by one-way ANOVA (statistical significance set at $p < 0.05$). Bacterial motility in the presence of different DsbA inhibitor concentrations was plotted as % motility over concentration (M) by measuring the diameter of the motility zone in plates containing 0.005, 0.05, 0.1, or 1 mM inhibitors and dividing by the diameter of the same strain swimming in DMSO-containing media (carrier control).

Declaration of Competing Interest

The authors declare that they have no known competing financial interests or personal relationships that could have appeared to influence the work reported in this paper.

Acknowledgments

This research was supported by National Health and Medical Research Council (NHMRC) project (grants 1099151 and 1144046) and the Australian research council (Future Fellowship (FT130100580) and Discovery Project (DP190101613)). Dr Luke Duncan would like to acknowledge La Trobe University as a recipient of La Trobe University Postgraduate Research Scholarship. Dr Makrina Totsika would like to acknowledge support from Queensland University of Technology as a recipient of a Vice-Chancellor's Research Fellowship. We would also like to acknowledge the La Trobe University-Comprehensive Proteomics Platform and the Monash Fragment Platform (MFP) for providing infrastructure and expertise. This research was undertaken on the MX1 and MX2 beamlines at the Australian Synchrotron, part of Australian Nuclear Science and Technology Organisation (ANSTO). We are very grateful for the ongoing support and many helpful chemical discussions provided by Dr Les Deady.

Appendix A. Supplementary material

Supplementary data to this article can be found online at https://doi.org/10.1016/j.bmc.2021.116315.

References

1 World Health Organization, Antimicrobial resistance: global report on surveillance; 2014.
2 World Health Organization, 2019 antibacterial agents in clinical development: an analysis of the antibacterial clinical development pipeline; 2019.
3 Totsika M. Disarming pathogens: benefits and challenges of antimicrobials that target bacterial virulence instead of growth and viability. *Future Med Chem*. 2017;9:267–269.
4 Heras B, Scanlon MJ, Martin JL. Targeting virulence not viability in the search for future antibacterials. *Br J Clin Pharmacol*. 2015;79:208–215.
5 Dickey SW, Cheung GYC, Otto M. Different drugs for bad bugs: antivirulence strategies in the age of antibiotic resistance. *Nat Rev Drug Discov*. 2017;16:457–471.
6 Casadevall A, Pirofski LA. Host-pathogen interactions: redefining the basic concepts of virulence and pathogenicity. *Infect Immun*. 1999;67:3703–3713.
7 Heras B, Shouldice SR, Totsika M, Scanlon MJ, Schembri MA, Martin JL. DSB proteins and bacterial pathogenicity. *Nat Rev Microbiol*. 2009;7:215–225.
8 Landeta C, Boyd D, Beckwith J. Disulfide bond formation in prokaryotes. *Nat Microbiol*. 2018;3:270–280.

9 Shouldice SR, Heras B, Walden PM, Totsika M, Schembri MA, Martin JL. Structure and Function of DsbA, a Key Bacterial Oxidative Folding Catalyst. *Antioxid Redox Signal*. 2011;14:1729–1760.
10 Smith RP, Paxman JJ, Scanlon MJ, Heras B. Targeting Bacterial Dsb Proteins for the Development of Anti-Virulence Agents. *Molecules*. 2016;21:811–825.
11 Martin JL, Bardwell JCA, Kuriyan J. Crystal structure of the DsbA protein required for disulphide bond formation in vivo. *Nature*. 1993;365:464–468.
12 Inaba K, Murakami S, Suzuki M, et al. Crystal structure of the DsbB-DsbA complex reveals a mechanism of disulfide bond generation. *Cell*. 2006;127:789–801.
13 Duprez W, Premkumar L, Halili MA, et al. Peptide inhibitors of the *Escherichia coli* DsbA oxidative machinery essential for bacterial virulence. *J Med Chem*. 2015;58:577–587.
14 Adams LA, Sharma P, Mohanty B, et al. Application of Fragment-Based Screening to the Design of Inhibitors of *Escherichia coli* DsbA. *Angew Chem, Int Ed*. 2015;54:2179–2184.
15 Totsika M, Vagenas D, Paxman JJ, et al. Inhibition of Diverse DsbA Enzymes in Multi-DsbA Encoding Pathogens. *Antioxid Redox Signal*. 2018;29:653–666.
16 Bardwell JCA, McGovern K, Beckwith J. Identification of a protein required for disulfide bond formation in vivo. *Cell*. 1991;67:581–589.
17 Lamoree B, Hubbard RE. Current perspectives in fragment-based lead discovery (FBLD). *Essays Biochem*. 2017;61:453–464.
18 Kirsch P, Hartman AM, Hirsch AKH, Empting M. Concepts and Core Principles of Fragment-Based Drug Design. *Molecules*. 2019;24:4309–4330.
19 Duncan LF, Wang G, Ilyichova OV, Scanlon MJ, Heras B, Abbott BM. The fragment-based development of a benzofuran hit as a new class of *Escherichia coli* DsbA inhibitors. *Molecules*. 2019;24:3756–3782.
20 Mayer M, Meyer B. Characterization of Ligand Binding by Saturation Transfer Difference NMR Spectroscopy. *Angew Chem, Int Ed*. 1999;38:1784–1788.
21 Carr HY, Purcell EM. Effects of Diffusion on Free Precession in Nuclear Magnetic Resonance Experiments. *Phys Rev*. 1954;94:630–638.
22 Dalvit C, Fogliatto G, Stewart A, Veronesi M, Stockman B. WaterLOGSY as a method for primary NMR screening: Practical aspects and range of applicability. *J Biomol NMR*. 2001;21:349–359.
23 Hubbard RE, Murray JB. Chapter twenty - Experiences in Fragment-Based Lead Discovery. In: Kuo LC, ed. *Methods Enzymol*. Academic Press; 2011:509–531.
24 Bentley MR, Ilyichova OV, Wang G, et al. Rapid Elaboration of Fragments into Leads by X-ray Crystallographic Screening of Parallel Chemical Libraries (REFiLX). *J Med Chem*. 2020;63:6863–6875.
25 Kadokura H, Tian H, Zander T, Bardwell JC, Beckwith J. Snapshots of DsbA in action: detection of proteins in the process of oxidative folding. *Science*. 2004;303:534–537.
26 Paxman JJ, Borg NA, Horne J, et al. The structure of the bacterial oxidoreductase enzyme DsbA in complex with a peptide reveals a basis for substrate specificity in the catalytic cycle of DsbA enzymes. *J Biol Chem*. 2009;284:17835–17845.
27 Verderosa AD, Dhouib R, Hong Y, Anderson TK, Heras B, Totsika M. A high-throughput cell-based assay pipeline for the preclinical development of bacterial DsbA inhibitors as antivirulence therapeutics. *Sci Rep*. 2021;11:1569–1581.
28 Armarego WLF, Chai CLL. Chapter 4 - Purification of Organic Chemicals. In: Armarego WLF, Chai CLL, eds. *Purification of Laboratory Chemicals (Fifth Edition)*. Burlington: Butterworth-Heinemann; 2003:80–388.
29 Theodorou V, Skobridis K, Tzakos AG, Ragoussis V. A simple method for the alkaline hydrolysis of esters. *Tetrahedron Lett*. 2007;48:8230–8233.
30 McPhillips TM, McPhillips SE, Chiu HJ, et al. Blu-Ice and the Distributed Control System: software for data acquisition and instrument control at macromolecular crystallography beamlines. *J Synchrotron Radiat*. 2002;9:401–406.
31 Battye TGG, Kontogiannis L, Johnson O, Powell HR, Leslie AGW. iMOSFLM: A new graphical interface for diffraction-image processing with MOSFLM. *Acta Crystallogr, Sect D: Biol Crystallogr*. 2011;67:271–281.
32 Kabsch W. Software XDS for image rotation, recognition and crystal symmetry assignment. *Acta Crystallogr, Sect D: Biol Crystallogr*. 2010;66:125–132.
33 Evans PR, Murshudov GN. How good are my data and what is the resolution? *Acta Crystallogr, Sect D: Biol Crystallogr*. 2013;69:1204–1214.
34 Bailey S. The CCP4 suite: programs for protein crystallography. *Acta Crystallogr, Sect D: Biol Crystallogr*. 1994;D50:760–763.
35 McCoy AJ, Grosse-Kunstleve RW, Adams PD, Winn MD, Storoni LC, Read RJ. Phaser crystallographic software. *J Appl Crystallogr*. 2007;40:658–674.
36 Guddat LW, Bardwell JCA, Glockshuber R, Huber-Wunderlich M, Zander T, Martin JL. Structural analysis of three His32 mutants of DsbA: support for an electrostatic role of His32 in DsbA stability. *Protein Sci*. 1997;6:1893–1900.
37 Emsley P, Cowtan K. Coot: model-building tools for molecular graphics. *Acta Crystallogr, Sect D: Biol Crystallogr*. 2004;D60:2126–2132.
38 Adams PD, Afonine PV, Bunkoczi G, et al. PHENIX: a comprehensive Python-based system for macromolecular structure solution. *Acta Crystallogr, Sect D: Biol Crystallogr*. 2010;66:213–221.
39 Ziarek JJ, Peterson FC, Lytle BL, Volkman BF. Binding site identification and structure determination of protein-ligand complexes by NMR: A semiautomated approach. *Methods Enzymol*. 2011;493:241–275.
40 Kurth F, Rimmer K, Premkumar L, et al. Comparative sequence, structure and redox analyses of Klebsiella pneumoniae DsbA show that anti-virulence target DsbA enzymes fall into distinct classes. *PloS One*. 2013;8(11):e80210.
41 Totsika M, Heras B, Wurpel DJ, Schembri MA. Characterization of Two Homologous Disulfide Bond Systems Involved in Virulence Factor Biogenesis in Uropathogenic *Escherichia coli* CFT073. *J Bacteriol*. 2009;191:3901.
42 Auld Douglas, Inglese James, Dahlin Jayme. In: Markossian S, Grossman A, Brimacombe K, et al., eds. *Assay Guidance Manual*. Bethesda (MD): Eli Lilly & Company and the National Center for Advancing Translational Sciences; 2004. https://www.ncbi.nlm.nih.gov/books/NBK442297/.